

Gizem Karsli Uzunbas, Faraz Ahmed, and Morgan A. Sammons\*

Department of Biological Sciences, State University of New York at Albany, Albany, NY 12222

*RUNNING TITLE: p63 controls enhancer identity and p53 activity*

\* To whom correspondence should be addressed. Tel: 518-442-4526; Fax: 518-442-4767; Email: masammons@albany.edu

**Keywords:** transcription, transcription factor, transcription regulation, chromatin modification, chromatin regulation, chromatin, p53, p63, DNA damage response, epigenetics

## ABSTRACT

Transcriptional activation by p53 provides powerful, organism-wide tumor suppression. We hypothesized that the local chromatin environment, including differential enhancer activities, contributes to various p53-dependent transcriptional activities in different cell types during stress-induced signaling. In this work, using ChIP-seq, immunoblotting, qPCR, and computational analyses across various mammalian cell lines, we demonstrate that the p53-induced transcriptome varies by cell type, reflects cell type-specific activities, and is considerably broader than previously anticipated. We found that these molecular events are strongly influenced by p53's engagement with differentially active cell type-specific enhancers and promoters. We also observed that p53 activity is dependent on the p53 family member tumor protein p63 in epithelial cell types. Notably, we demonstrate that p63 is required for epithelial enhancer identity including enhancers used by p53 during stress-dependent signaling. Loss of p63, but not p53, caused site-specific depletion of enhancer-associated chromatin modifications, suggesting that p63 functions as an enhancer maintenance factor in epithelial cells. Additionally, a subset of epithelial-specific enhancers is dependent on the activity of p63 providing a direct link between lineage determination and enhancer structure. These results suggest that a broad, cell-intrinsic mechanism controls p53-dependent cellular stress response through differential regulation of *cis*-regulatory elements.

## INTRODUCTION

The p53 family of transcription factors regulates highly diverse cellular functions, including tumor suppression and control of cell specification and identity (1). p53 is a master tumor suppressor that protects organismal fidelity after exposure to cellular stress like DNA damage. This activity is dependent on p53's ability to activate transcription of a canonical network of genes involved in DNA damage repair, cell cycle arrest, apoptosis, and senescence (2).

Many of these canonical transcriptional pathways are individually dispensable for tumor suppression, suggesting p53 regulates a redundant and not yet fully characterized transcriptional network (3, 4).

Genetic inactivation of the p53 tumor suppressor is highly recurrent across cancer types. p53 mutations, while frequent, vary depending on the tumor type with additional genetic and epigenetic mechanisms proposed to inactivate the p53 pathway in the presence of

wild-type p53 (5–7). p63 and p73, p53 family members, function similarly to p53 in stress response, although their precise roles in tumor suppression are unresolved (8–10). p63 and p73 are primarily lineage restricted to epithelial cell types where each serves critical and non-overlapping roles in cell identity and self-renewal (1, 11). Mutations in TA- and  $\Delta$ N-p63 isoforms of p63 are causative for a number of epithelial-associated human developmental disorders independent of p53 activity, and mutations in p63 target genes underlie similar phenotypes (12, 13). A significant and still outstanding question involves dissection of specific roles and functional interplay between p53 family members during development, in the regulation of cellular homeostasis, and in the etiology of disease.

The similarity between DNA binding motifs originally suggested that competition for binding sites might play a central role in the regulation of p53 family member activity (14–16). Indeed, previous studies implicate the  $\Delta$ N-p63 isoforms, lacking a canonical transactivation domain, as direct repressors of the p53-induced transcriptome through a binding site competitive mechanism (17–19). Multiple p63-dependent mechanisms repressing p53 activity have been identified, including control of H2AZ deposition and HDAC recruitment (20–23). Increased p63 activity is thought to drive certain epithelial-derived cancers, particularly squamous cell carcinomas, with both p53-dependent and independent mechanisms (24). As the majority of cancers are derived from epithelial tissues, the mechanisms of p53 family dependent tumor suppression in those tissues is of special interest (7).

Fate choice after p53 activation, be it apoptosis, temporary/permanent cell cycle arrest, or continued proliferation, is variable across cell types suggesting that p53-dependent transcription is also cell type-dependent (2). A bevy of sensitive methodological approaches have been used to identify p53 binding sites and gene targets across transformed and primary cell lines in an effort to explain these terminal cell fate choices and p53-dependent tumor suppression.

A recent set of meta-analyses have suggested that p53 binding to the genome is invariant (25), proposing that p53 acts independently to drive gene expression of a core tumor suppressor network across all cell types due to the low enrichment of other transcription factor motifs at p53-bound enhancers and the reported pioneer factor activity of p53 (3, 25, 26). Conversely, a series of recent p53 ChIP-seq experiments observed cell type-specific p53 binding and gene targets (27, 28). Because of the high importance of these conflicting observations and the mutual exclusivity of the models, additional experimental evidence and models are required to unravel these disparate p53 regulatory mechanisms.

We previously proposed that the local chromatin environment, including variable chromatin accessibility and enhancer activity, contributes to novel p53 activities across cell types (29). To address this question, we performed genomewide transcriptome, epigenome, and p53 cistrome profiling in primary foreskin fibroblasts (SkFib) and mammary basal epithelial (MCF10A) cell lines, two cell types with varying enhancer activity at p53 binding sites (29). Our results directly implicate differential *cis*-regulatory element activity as a mediator of the p53 network, with both differential promoter and enhancer activity contributing to p53-dependent gene expression variability. Further, we have identified the p53 family member p63 as one factor that drives the epithelial-specific p53 transcriptome through an enhancer maintenance activity. We further propose that p63 serves as a pioneer factor for a set of epithelial-specific enhancers. Thus, these data support a mechanism whereby co-operating transcription factors control cell type-dependent *cis*-regulatory networks that regulate p53 activity.

## RESULTS

### **p53-dependent activation of conserved and cell type-specific transcription.**

Gene activation downstream of p53 stabilization has been extensively studied, but

whether p53 transcriptionally activates the same genes across all cell types is still unresolved. Previous work suggested that p53-dependent transcriptional activity might vary between epithelial cells and fibroblasts due to differences in predicted enhancer activity between the two cell types (29). We chose two widely used model cell lines (MCF10A mammary epithelial cells and dermal foreskin fibroblasts) to address this unresolved question. The two cell types differ in developmental origin, with dermal fibroblasts and mammary epithelial cells arising from mesoderm and ectoderm, respectively. Importantly, both cell types are non-tumorigenic in mouse models, suggesting they represent a non-transformed state.

We performed three biological replicates of polyA-enriched, strand-specific RNA-seq in both cell lines after p53 activation in response to a 6 hour treatment with 5 $\mu$ M Nutlin-3A. Nutlin-3A is a highly-specific MDM2 antagonist that leads to p53 stabilization without activation of p53-independent DNA damage pathways that can confound analysis (38, 39). Raw data were aligned using STAR and differentially expressed genes were called using DESeq2. Use of a stringent cutoff (2-fold increase in expression after Nutlin-3A treatment, q-value<0.05) revealed different patterns of gene expression for MCF10A versus SkFib (Figure 1A). Genes upregulated in both cell lines are significantly associated with the core p53 response and programmed cell death (Figure 1B, Supplemental Table S1), as expected. MCF10A displayed a larger group of Nutlin-3A-induced targets enriched in gene ontology groups related to establishment of the epithelial barrier and p53-dependent processes like programmed cell death and homeostasis (Figures 1A-B). SkFib showed a markedly smaller, albeit specific, p53-activated transcriptome (Figure 1A). These genes are associated with other cell stress-related pathways including those associated with the hypoxia response and catabolic processes. Allowing for any change in expression while maintaining a corrected p-value of less than 0.05 yielded an increased number of commonly and differentially regulated genes, but the trend that

p53-dependent gene targets are more abundant in MCF10A cells remained consistent across analyses methods (Supplemental Figure S1A).

Orthogonal validation by qRT-PCR confirmed a stringent cell type-specificity for the tested set of genes identified by RNA-seq (Figures 1C-E). Upregulation of canonical p53 targets like *BTG2* and *CDKN1A* are indeed similar across cell types (Figure 1C). Many of the cell type-specific targets were undetected or detected at extremely low levels in the opposing cell type (Figures 1D-E). The majority of the MCF10A-specific targets represent novel p53-dependent genes not previously identified in a large-scale meta-analysis of human p53 gene targets (32). Over 20% of newly identified SkFib-specific targets have not been observed previously (Figure 1F, Supplemental Tables S2-3). These initial analyses reveal that the p53-activated transcriptome varies between non-transformed cell types and may reflect tailored, cell type-dependent responses after cellular stress. In order to confirm the p53-dependent nature of these Nutlin-3A-induced genes, p53 mRNA and protein expression were depleted using shRNA in both MCF10A and SkFib (Figures 1G-H and 1J-K). Knockdown of p53 in SkFib (Figure 1G-H) led to sharp reduction in both basal and Nutlin-3A-induced expression of the SkFib-specific genes, *GDNF* and *TRIM55* (Figure 1I). Depletion of p53 in MCF10A (Figures 1J-K) caused a loss of Nutlin-3A-induced *R/C3* and *IL1B* expression relative to a non-targeting control shRNA (Figure 1L). Taken together, our RNA-seq analysis and p53-depletion experiments indicate differential activation of p53-dependent targets across non-transformed cell lines.

### Differential genomic binding of p53 between mesenchymal and epithelial cell types.

The most straightforward potential mechanism driving our observation of cell type-dependent transcriptional activation by p53 involves differential binding of p53 to regulatory

regions controlling those genes. Recent analyses reached opposing conclusions with regard to the cell type-dependence of p53 engagement with the genome (3, 25, 27, 28). We therefore assessed whether differences in p53 engagement with the genome in our model cell lines might explain our observations of cell type-dependent transcriptomes. Two biological replicates of p53 ChIP-seq were performed in either DMSO or Nutlin-3A-treated MCF10A and SkFib. Regions of significant p53 enrichment relative to input (peaks) were called using MACS2 (33). Only peaks identified in both replicates were considered for further analysis (see Materials and Methods). Consistent with the cell type-dependence of our gene expression observations, our ChIP-seq approach revealed a highly-enriched set of MCF10A-specific p53 binding sites and a smaller number of SkFib-specific sites (Figure 2A). A highly-similar set of differential p53 binding events was also observed using the DiffBind statistical framework (Supplemental Figure S1B), suggesting the differential binding is unlikely to be an artifact of any one peak calling or replication strategy. Taken together, our peak calling approaches indicate differential genome engagement of p53 in MCF10A versus SkFib.

At commonly bound sites, basal and Nutlin-3A-induced p53 enrichment is higher in MCF10A relative to SkFib (Figure 2B). Despite higher overall occupancy in MCF10A, SkFib show higher relative fold-change in p53 enrichment between DMSO and Nutlin-3A treatment (Figure 2B). Relatedly, absolute p53 occupancy differences do not correlate with the ability to activate common gene targets as Nutlin-3A induced gene fold-changes are higher in SkFib compared to MCF10A (Figure 2C). Cell type-specific binding events displayed lower absolute p53 occupancy than at common sites, suggesting that common sites might represent more stable or higher affinity p53 binding sites (Figures 2B,D-E). This observation is in line with previous observations in transformed cancer cell lines and suggests a core set of p53 binding

events is well conserved across cell types (3, 25, 27).

We then wanted to validate our observations of differential p53 binding using standard ChIP-qPCR methods. p53 binding at the CDKN1A promoter in both MCF10A and SkFib increased in response to Nutlin-3A treatment and was sensitive to depletion of p53 by shRNA (Figure 2F). ChIP signal at the CDKN1A promoter was more highly enriched relative to a region  $\approx$ 4kb upstream of the binding event, confirming the specificity of p53 binding. Examination of p53 binding at two genomic locations in SkFib and MCF10A confirmed our ChIP-seq studies. p53 binding was enriched at the *BDNF* locus in SkFib and was sensitive to p53 depletion, whereas the signal observed in MCF10A was at a background level and not affected by either Nutlin-3A treatment or p53 knockdown (Figure 2G). Similar cell type-specificity was observed for an MCF10A-specific p53 binding event (Figure 2H). Taken together, these data provide evidence that the p53-dependent transcriptome is cell type-specific and that p53 engagement with the genome is variable across cell types.

### Promoter and enhancer chromatin states correlate with differential p53 binding and transcriptional activity.

We next wanted to identify potential mechanisms driving cell type-specificity within the p53-dependent transcriptome and cistrome. Previous analyses of p53 genomic occupancy suggested that gene proximal binding of p53 correlates with changes in gene activation (3, 32), but that many p53-dependent gene targets are likely regulated by more distal p53 binding events. MCF10A-specific genes are more likely to have a p53 binding event near their TSS compared to p53 peaks in SkFib (Supplemental Figure S1C). Conversely, SkFib-specific genes are not associated with either a higher number of SkFib-specific p53 binding events or more proximal p53 binding events than in MCF10A (Supplemental Figure S1C). These observations suggest that while cell type-specific p53 binding correlates with an increase in p53 gene targets in

MCF10A, differential p53 binding alone is insufficient to explain differential gene expression. We and others previously proposed that differential regulatory region activity may control p53-dependent gene expression (29, 34), and enhancers and promoters have a well-known and strong cell type-dependence (35, 36). Therefore, we performed ChIP-seq experiments for canonical promoter (H3K4me3) and enhancer-associated (H3K4me2, H3K27ac) histone modifications to determine whether differentially active promoters or enhancers might explain the observed cell type specificity of the p53 transcriptome and cistrome. Experiments were performed under both DMSO and Nutlin-3A-treated conditions to observe any p53-associated changes in local chromatin modification state.

We first examined the genomic context surrounding *GDNF*, a SkFib-specific p53-dependent target gene (Figure 11). We observed a proximal p53 binding event 8.5kb from the *GDNF* transcriptional start site (Figure 3A, dashed box) in both SkFib and MCF10A. This binding site is enriched for H3K27ac but devoid of H3K4me3, suggesting this region might be active as an enhancer in both cell types. The *GDNF* promoter is strongly enriched for the canonical promoter-associated histone modification H3K4me3 as well H3K4me2 and H3K27ac in SkFib (solid box, Figure 3A). These modifications are either substantially diminished or absent from the *GDNF* promoter in MCF10A. These observations suggest that differential promoter activity may be one mechanism by which cell types permit activation of particular p53 target genes without changes in p53 genomic occupancy.

We next investigated putative mechanisms driving our observation of epithelial-specific p53 target gene activation. p53 binds to more genomic locations and is found closer to cell type-specific, regulated genes in MCF10A relative to SkFib (Figure 2A, Supplemental Figure S1C), suggesting that these binding events might explain the expansion of p53-dependent genes in MCF10A cells. Examination of the MCF10A-

specific target *RIC3* revealed MCF10A-specific binding of p53 to a putative intragenic enhancer (Figure 3B, dashed box). This putative enhancer region, characterized by enrichment of H3K4me2 and H3K27ac and depletion of H3K4me3, appeared specific to MCF10A. Globally, MCF10A-specific p53 binding occurred within regions that are strongly enriched for this chromatin modification-based signature of transcriptional enhancers (Figures 4A-C, E). These MCF10A-specific p53 binding sites show little evidence of p53 occupancy and lack enrichment of H3K27ac and H3K4me2 in SkFib (Figures 4A, E). The lack of enhancer-associated chromatin modifications is not a general feature of SkFib, as common p53 binding events show similar enrichment of H3K27ac and H3Kme2 in both SkFib and MCF10A, and SkFib-specific p53 sites are enriched for H3K27ac relative to MCF10A (Figures 4D, F and Supplemental Figure S1D). These data suggest that differential enrichment of enhancer-associated chromatin modifications correlates with cell type-specific p53 binding but that multiple mechanisms, like differential promoter activity, may also regulate cell type-specific p53 gene targets.

#### **ΔN-p63 $\alpha$ co-occupies the majority of MCF10A-specific p53 binding sites.**

Our data point towards differential enhancer accessibility and/or activity as a potential driver of differential p53 binding and activity across cell types. Enhancer specification, activity, and histone modifications are generally thought to be regulated by the combined effort of both common and lineage-dependent transcription factors (36). Multiple recent reports suggest that p53 activity at *cis*-regulatory elements is independent of any accessory transcription factors, primarily due to low enrichment/specification of other DNA motifs (25, 26, 34). We sought to examine what factors, if any, might regulate accessibility and chromatin modification patterns observed at differentially enriched or regulated p53 binding sites. We compared transcription factor motif enrichment at MCF10A-specific putative enhancers (defined as

H3K27ac+/H3K4me2+/H3K4me3- regions) compared to SkFib-specific enhancers using HOMER. We observed no enrichment of any specific transcription factor motifs in SkFib-specific enhancers relative to MCF10A (Figure 5A, Supplemental Table S4). Conversely, MCF10A-specific enhancers are enriched in motifs for p53 family members, including both p53 and p63 (Figure 5A, Supplemental Table S4). These motif enrichment data are consistent with results from the FANTOM consortium showing that enhancers within other epithelial cell types are enriched for p53 family transcription factor motifs (37). As the p53 family shares a common, although not identical, response element motif, we asked whether p53 or other family members might regulate MCF10A-specific p53 binding events, enhancer-associated chromatin modifications, and p53-dependent gene expression.

Basal epithelial cells like MCF10A are known to specifically express p63 and are dependent on p63 activity for self-renewal and epidermal commitment *in vivo* (38). p63 also bookmarks enhancers during epidermal differentiation (39) and regulates chromatin accessibility through interactions with chromatin modifiers (40–44). As p53 is expressed in all cell types and p73 is most abundant in ciliated cell types (45, 46), we focused on p63 as a potential mediator of our observations of a unique p53-dependent transcriptome in MCF10A. We confirmed the expression of p63 mRNA and absence of p73 using RT-qPCR (Figure 5B). Two N-terminal p63 isoforms (TA and  $\Delta$ N) can be produced from alternative promoters and have non-overlapping roles (9). The TA isoform encodes a longer protein containing a transcriptional activation domain, whereas the  $\Delta$ N isoform lacks a canonical activation domain. TA-p63 activates expression of a number of p53 target genes upon DNA damage and is involved in the late stages of squamous epithelial cell differentiation (47).  $\Delta$ N-p63 was originally thought to be inhibitory, as it lacks an activation domain, but is now understood to act in both gene activating and repressing manner through

cofactor recruitment (18). We found that the  $\Delta$ N-p63 mRNA isoform, and not TA-p63, is expressed in MCF10A (Figure 5C). Western blot analysis using N-terminal isoform-specific antibodies further confirmed expression of  $\Delta$ N-p63 and undetectable levels of the TA isoform (Figures 5D-E). The p63 mRNA can also be alternatively spliced to produce multiple C-terminal variants. We used a p63 $\alpha$ -specific antibody which targets a unique region of the longest C-terminal variant; thus, our analysis is restricted to characterization of the  $\Delta$ N-p63 $\alpha$  isoform (hereby referred to as p63 for clarity).

We then asked whether p63 might be involved in p53-dependent gene activation in MCF10A by performing genomewide ChIP-seq of p63 in MCF10A following DMSO or Nutlin-3A treatment. Examination of *IL1B* and *RNASE7*, MCF10A-specific p53 targets, revealed p63 binding to distinct enhancer regions co-occupied by p53 in an MCF10A-specific manner (Figures 5F-G). These p53/p63 binding sites have strong enhancer-associated enrichment of H3K27ac and H3K4me2 that is absent in SkFib. Globally, p63 binds to significantly more genomic loci than does p53 (Figure 5H), and nearly 60% of epithelial-specific p53 binding events overlap regions of p63 binding (Figure 5H). p53 and p63 enrichment at shared binding sites is highly similar (Figure 5I). Regions occupied by both p53 and p63 are more likely to be enriched with enhancer-associated chromatin modifications (H3K27ac and H3K4me2) than locations bound by only p53 (Figure 5J), suggesting p63 binding might increase enhancer activity. Consistent with this, sites bound by only p63 are more likely than even p53/p63 co-occupied sites to be putative enhancer regions based on their chromatin modification enrichment patterns (Figure 5J). More p63 binding events occur within 10kb of the TSS of Nutlin-3A-induced MCF10A genes relative to all other genes, providing additional evidence that that p63 might co-regulate these specific target genes (Figure 5K). These data provide evidence that p63 occupies p53-bound, putative enhancers in MCF10A basal epithelial cells.

## Co-regulation of p53-dependent MCF10A target genes by p63

In order to test whether p63 regulates p53 activity, we created MCF10A cells stably-expressing shRNA targeting the DNA binding domain common to all potential p63 isoforms. p63 expression was reduced at the RNA level compared to control non-targeting (scr) shRNA (Figure 6A), and was nearly absent at the protein level (Figure 6B). Knockdown of p53 surprisingly led to an increase in p63 mRNA expression, with a similar reciprocal regulation observed for increased p53 expression in p63 knockdown experiments (Figure 6A). We then performed RNA-seq analysis of MCF10A cells expressing non-targeting (scr), p53, or p63 shRNA to determine their relative contributions to p53-dependent and MCF10A-specific target genes. Loss of p53 expression strongly inhibited expression of the previously identified Nutlin-3A-induced MCF10A-specific genes, consistent with this set of genes representing p53 dependent targets (Figure 6C). Globally, Nutlin-3A-induced target gene activation is inhibited by p63 knockdown relative to non-targeting controls, suggesting p63 activity is required for a set of MCF10A p53 targets (Figure 6C). Overall, 40% of p53 target genes are sensitive to knockdown of p63 (Supplemental Figure S1E). The remainder of the genes are either unaffected (47%) or have more robust p53-dependent transactivation after p63 depletion (12%), suggesting that p63 represses a subset of p53-target genes.

Our data suggest that p63 can co-activate or repress a set of p53-dependent genes in epithelial cell types. We confirmed these RNA-seq results by qRT-PCR on a panel of epithelial target genes after p53 or p63 knockdown. *R/C3*, previously demonstrated to be a p53-dependent gene (Figure 1L), is de-repressed in the absence of p63, suggesting p63 might partially repress this target gene (Figure 6D). Conversely, both *IL1A* and *IL1B* are dependent on p53 and p63 for full transactivation, with *IL1B* showing a strong dependence on p63 for basal expression (Figure

6D). Overall, knockdown of p63 also led to basal gene expression changes for p53 targets and non-p53-dependent genes related to cell cycle and cell adhesion/extracellular matrix (Supplemental Table S5), as has previously been described in p63 perturbation experiments (48). In total, these results suggest that p63 functions as both a co-activator and repressor of p53-dependent transcription in MCF10A, but how these opposing mechanisms lead to differential p53 activity requires further inquiry.

Given that p63 appears to have both positive and negative roles in p53-dependent gene expression, we sought additional insight into the roles of p53 and p63 bound genomic elements with respect to p63-activated or repressed genes. We binned p53-bound, p63-bound, and p53/p63 co-bound sites into groups of either less than or greater than 25kb from the TSS of p53-dependent genes. These genes fell into three categories based on their behavior after p63 knockdown, p63-dependent, p63-independent, or p63-repressed. Genes requiring both p53 and p63 for full Nutlin-3A-mediated expression are more likely to have a p53/p63 co-bound site within 25kb of its TSS than the genomewide average ( $p<0.0001$ , chi-square test, Figure 6E). p63-dependent p53 targets are not associated with p63-only sites ( $p=0.1389$ ). Similarly, p63-independent p53 targets are actually further away from p63 only binding sites than expected ( $p=0.0123$ , chi-square test, Figure 6E). Importantly, p63-inhibited p53 targets are highly likely to be within 25kb of a p53/p63 co-binding event ( $p<0.0001$ , chi-square test), but not sites bound by just p63 ( $p=0.4238$ , chi-square test). These results are consistent with reports of multiple p63-mediated transcriptional repression mechanisms such as direct binding site competition, HDAC recruitment, and H2AZ deposition (18–23), although defining the specific mechanisms at play, and whether multiple p63-dependent activities work in combination or exclusively, requires further experimentation.

## p53 activity is necessary for stimulus-dependent, but not basal, enrichment of histone modifications at p53 binding sites

Our results suggest that p63 activity is required for p53-dependent induction of a group of target genes in MCF10A basal breast epithelial cells. p53 and p63 engagement to the genome in epithelial cells correlates with enhancer-associated histone modifications and p63 appears to be required for full expression of a number of p53 gene targets (Figure 6C-D). We sought to further extend our analysis of the role of p63 in p53 target gene expression in MCF10A basal epithelial cells. The p53 family are putative pioneer factors with enhancer bookmarking and licensing activity (29, 39, 40, 49, 50). Therefore, we examined whether p53 or p63 activity might influence chromatin modification dynamics at putative enhancers.

A number of studies have demonstrated that p53 has pioneer factor activity as it can directly bind its consensus sequence in the context of a nucleosome (29, 51, 52). Whether p53 can mediate chromatin accessibility and the deposition of stereotypical enhancer and promoter-associated chromatin modifications is more controversial. Indeed, the large majority of p53 binding sites are constitutively closed or are within previously accessible chromatin (3, 26, 29), but recent reports suggest p53 might have a context-dependent ability to mediate chromatin accessibility (26). Therefore, we examined whether p53 might serve either pioneer or maintenance roles at enhancers. We examined H3K4me2 and H3K27ac enrichment at p53 binding sites using ChIP-seq in control, p53, or p63 targeting shRNA MCF10A cells. Basal, unstimulated H3K4me2 and H3K27ac enrichment at p53 binding sites was largely unaffected by the loss of p53 (Figures 7A-B), although the decrease in H3K27ac after p53 depletion is statistically significant. Nutlin-3A treatment and p53 stabilization led to a marked increase in H3K4me2 and H327ac relative to basal levels (Figures 7A-B), with almost 20% of all p53 binding sites displaying a 2-fold or greater

increase in H3K27ac after p53 binding (Figure 7C). The gain in H3K4me2 and H3K27ac after Nutlin-3A treatment at p53 binding sites is substantially reduced upon p53 knockdown (Figures 7A-B), suggesting this process is highly dependent on local p53 binding and recruitment of histone modifying machinery. These data are consistent with previous reports of p53-dependent gains in enhancer and promoter-associated chromatin modifications at regulatory regions (29).

Unlike our results with p53, p63 knockdown led to a reduction of H3K27ac and H3K4me2 enrichment at p53 binding sites (Figures 7A-B) before p53 stabilization with Nutlin-3A. Additionally, the absence of p63 led to a marked increase in H3K27ac at p53 binding sites (Figure 7C) after Nutlin-3A treatment. Overall, nearly 85% of all p53 binding sites in MCF10A displayed over a 2-fold increase in H3K27ac enrichment relative to DMSO in the absence of p63 (Figure 7C). This increase in H3K27ac is observed at non-p53-bound enhancers as well, suggesting p63 might normally dampen H3K27ac enrichment at enhancers. This would be consistent with reports of p63-dependent recruitment of HDAC1 and HDAC2 to specific loci (22, 23). p53-bound enhancers that gain H3K27ac after p63 depletion are more likely to be co-bound by p63 ( $p<0.0001$ , chi-square, Supplemental Figure S1F) and nearer to p53-regulated genes than the sites unaffected by loss of p63 ( $p<0.0001$ , chi-square, Supplemental Figure S1G) suggesting this is a direct effect of p63 occupancy at those locations.

Epithelial cell types like MCF10A express multiple p53 family members that might redundantly regulate enhancer activity, making it difficult to assess the direct role of p53 in modulating enhancer activity. We therefore extended our analysis to isogenic WT or *TP53*-/-HCT116 human colon carcinoma cell lines and WT or *Trp53*-/- mouse embryonic fibroblasts (MEF). Both cell models lack endogenous p63 expression (HCT116, Figures 5D-E and MEF, Supplemental Figure S1H). This should allow us

to define the direct role of p53 in enhancer maintenance and activity. Similar to our observations in MCF10A cells, basal enhancer-associated H3K4me2 at p53-bound enhancers is unaffected by p53 deletion in HCT116 (Figure 7D). Unexpectedly, there is a slight increase in H3K4me2 enrichment after p53 loss. We also observe increased H3K4me2 enrichment at p53 binding sites after Nutlin-3A treatment, suggesting p53 does mediate recruitment or activation of local histone modifying enzymes (Figure 7D). Similarly, enrichment of H3K4me2 and H3Kme1, another transcriptionally-associated histone modification, does not decrease after p53 deletion (*Trp53<sup>-/-</sup>*) in mouse embryonic fibroblasts (MEFs) (Figure 7E). We do note a slight, but statistically significant, increase in H3K4me1 enrichment at potential p53 binding sites in *Trp53<sup>-/-</sup>* MEFs (Figure 7E). These data suggest that p53 is not an enhancer maintenance factor and contributes primarily to *de novo* histone acetylation and transcriptional activation at already established enhancers. These results suggest that p53 plays a limited role in the specification and maintenance of basal enhancer activity. The observed p53-independence of basal enhancer activity is consistent with previous observations that p53 is dispensable for basal eRNA abundance at enhancers (31).

### p63 regulates histone H3K4me2 and H3K27ac levels at p63-bound epithelial enhancers

p63, but not p53, depletion led to reduced enrichment of histone H3K27ac and H3K4me2 at p53-bound enhancers (Figures 7A-B). Recent genetic and biochemical evidence implicates p63 in establishment of enhancer chromatin structure during epithelial specification (39, 40, 42–44, 50). Therefore, we asked whether p63 activity was also required for maintaining the chromatin hallmarks of enhancer activity in MCF10A epithelial cells. Specifically, we measured H3K27ac and H3K4me2 levels at p63 binding sites in control or p63-depleted MCF10A epithelial cells. Overall, p63 depletion led to a reduction of H3K27ac and H3K4me2 at p63-

bound enhancers (Figures 8A-B). H3K4me2 levels at non-p63-bound enhancers are statistically different in p63 depleted cells relative to control experiments (paired t-test,  $p < 0.0001$ ), but the effect is not nearly as pronounced as at p63-bound enhancers (Figure 8B.) H3K27ac levels actually increase at non-p63-bound enhancers (Figure 8A). These results are consistent with multiple observations of p63-dependent HDAC recruitment to p63 binding sites (22, 23).

We then examined the *cis*-regulatory elements near *RRM1*, identified as a p63-dependent gene in our RNA-seq analysis, and *EDN2*, which was previously identified as a p63 target gene (20). p63-bound enhancers upstream of *RRM1* and *EDN2*, showed dramatic losses in both H3K27ac and H3K4me2 enrichment in p63-depleted cells (Figures 8C-D). We noted the loss of H3K4me2 and H3K27ac were specific for p63-bound enhancers and not putative promoter regions (Figure 8C). Additionally, not all p63-bound enhancers were affected by p63 depletion, as observed at the *EDN2* locus (Figure 8D, dashed boxes). In total, over 20% of H3K4me2+ and 15% of H3K27ac+ p63-bound sites showed at least a 2-fold depletion in MCF10A-p63sh cells relative to control shRNA (Figures 8E-F). These enhancer-associated histone modifications at p63 binding sites were generally unaffected by the loss of p53 (Figures 8E-F), suggesting this behavior is specific to p63. This loss of enhancer-associated histone modifications at p63 binding sites suggests that p63 plays a direct role in the establishment and maintenance of enhancer-associated histone modifications.

Our observations suggest that p63 activity is required for H3K27ac and H3K4me2 enrichment at a subset of its bound enhancers, but the stereotypical enhancer histone modification pattern (H3K4me2+/H3K27ac+) is not dependent on p63 at all p63-bound elements. Therefore, we classified p63-bound enhancers as either p63-dependent (greater than 2-fold decrease in H3K4me2 after p63 knockdown) or p63-independent (less than 2-fold). We

specifically chose to further investigate p63 binding sites with reduced H3K4me2 after p63 depletion, since p63 knockdown leads exclusively to a loss (and not gain) of this modification at p63 binding site (Figure 8F). Therefore, p63 is likely to be positively regulating the activity of these enhancers. p63-dependent enhancers are significantly more likely to overlap DNAse-hypersensitive sites (DHS) found in the 8 epithelial cell types of the ENCODE DHS Cluster set compared to non-epithelial cell types (Figure 8G, Supplemental Table S6). Similar results were observed when examining ChromHMM-based regulatory predictions for p63-dependent enhancers in epithelial and non-epithelial cell types (Supplemental Figure S11). Enhancers that were p63-bound, but whose chromatin modification states were unaffected by p63 loss, are more broadly accessible across cell types compared to the p63-dependent enhancers (Figure 8G). These data are consistent with p63 providing a pioneer factor-like role for a subset of its bound enhancers, as p63 expression is restricted to the epithelial lineage. As such, DNA accessibility and chromatin modification state at p63 independent enhancers are likely controlled by other, less cell type-restricted factors. Overall, p63 binding sites are strongly enriched for enhancer-associated modifications across epithelial cell types consistent with its well-established expression pattern and recently reported roles as a lineage determination and pioneer transcription factor (39, 42–44, 50).

Enhancer accessibility and activity is generally considered to be controlled by combinatorial transcription factor binding (53, 54); thus we used HOMER to examine enrichment of transcription factor motifs across p63-dependent and independent enhancers to identify additional transcription factors potentially regulating p63-bound enhancers (55). Both classes of p63-bound enhancers are enriched for p53/p63 and AP-1 family motifs (Figure 8H). Motifs for the AP-1 family are commonly enriched in enhancers (37, 56). p63-dependent enhancers are enriched for Smad family motifs in addition to a limited number of other enriched motifs like

HSF1, ZFX, and RFX2. p63-independent enhancers are strongly enriched for ETS family motifs relative to p63-dependent enhancers, with 20 different ETS family consensus motifs observed (Figure 8H, Supplementary Table S7), including the epithelial-specific member EHF. Numerous other motifs are enriched in p63-independent enhancers including Stat and Forkhead family motifs (Supplementary Table S7). These data are consistent with the broad chromatin accessibility of p63-independent enhancers observed across cell types (Figure 8G) and suggest that a subset of p63-bound regions depend on other transcription factors for DNA accessibility and enhancer-associated chromatin modifications. Our cell type-dependent DNA accessibility and transcription factor motif enrichment analyses suggest that p63 maintains or establishes chromatin structure at a set of epithelial-specific enhancers. Further, p63 binds to a series of enhancers whose accessibility is likely controlled by a series of other, non-epithelial-specific transcription factors.

## DISCUSSION

In this report, we focused on identifying mechanisms that control differential expression of p53 target genes across cell types. Our results demonstrate that differential *cis*-regulatory activity and p53 binding serve as critical determinants of cell type-specific, p53-dependent transcriptomes. The acute p53 response in foreskin fibroblasts (SkFib) and mammary epithelial cells (MCF10A) leads to distinct transcriptional programs that reflect cell type-specific functions. In the case of MCF10A, p53 activates a series of genes involved directly in epithelial cell identity, such as epithelial cornification genes and ZNF750, a key regulator of epithelial cell differentiation (57, 58). Knockout studies in mice suggest p53's role in epithelial development is limited, although neural tube and germ cell defects are observed at low penetrance (59–61). Therefore, our observations that p53 regulates key epithelial development and differentiation genes is surprising. Loss of p53

activity is a strong predictor of epithelial-to-mesenchymal transition (EMT) (62, 63). One potential rationale for p53-dependent regulation of these key epithelial lineage genes is a mechanism to protect against EMT by supporting transcription of epithelial identity genes. Of note, canonical p53 transcriptional pathways appear to be dispensable for tumor suppression (4), and the p53 transcriptional network is highly distributed as to allow loss of multiple target genes/pathways without overall loss of p53-dependent tumor suppression (3). Certainly, additional investigation into cell type-dependent p53 transcriptional targets, and their roles in context-dependent tumor suppression are warranted given these findings.

Our data suggest that transcriptional activation by p53 requires p53 binding to pre-established *cis*-regulatory elements. Fibroblast-specific p53 target genes have active promoters, characterized by canonical H3K4me3 enrichment, and p53 engagement with distal enhancer regions. Conversely, the same enhancers were active and engaged by p53 in MCF10A, but the gene promoters had chromatin-associated hallmarks of inactivity. It is currently unclear whether the lack of activity in MCF10A is driven by lack of promoter-bound cofactors, through repressive chromatin-associated mechanisms, or both. Repressive DNA and histone modifications have been implicated in differential control of p53 activity in cancer cell lines (64–66). Furthermore, the cell type-specific contribution of post-transcriptional mechanisms like RNA stability may contribute to the observed RNA differences (3), although these mechanisms have not been investigated here. Our observations suggest that promoter competence, independent of direct p53 binding, potently controls cell specific p53 transcription responses.

Although p53 is broadly expressed, distal p53-bound enhancers display significant differences in chromatin structure across cell types (29). p53 is a pioneer transcription factor capable of binding its response element within nucleosomal DNA (49, 51, 67), but whether p53

initiates chromatin remodeling after nucleosome binding is unclear. A recent ATAC-seq study in primary human skin fibroblasts demonstrated increased chromatin accessibility at a limited number of p53 binding sites after 12 hours of p53 activation with doxorubicin (26). In contrast, a shorter treatment with Nutlin-3A in human lung fibroblasts suggested p53 does not alter accessibility upon binding (29). Our results suggest that p53, which can bind to nucleosomal DNA *in vitro* and *in vivo*, does not broadly control enhancer chromatin accessibility. Genetic depletion of p53 in three model cell lines show no evidence for p53-dependent chromatin accessibility changes using the proxy of enhancer-associated chromatin modifications. Binding of p53, on the other hand, appears to substantially increase the enrichment of these histone modifications at enhancers, in agreement with a previous study (29). Taken together, these data and our observations suggest that p53's role in mediating enhancer accessibility may be context-dependent and depend on the presence of appropriate chromatin remodelers and other cofactors. This model requires the binding and activity of other transcription factors at p53-bound enhancers, which is a generally accepted model for enhancer establishment and activity. An alternative model was recently proposed where p53-dependent activity at regulatory regions like enhancers does not require the activity of additional transcription factors (25), which would make p53 a novel type of transcription factor working at enhancers. The p53-independent nature of chromatin accessibility and modification states at enhancers suggest that other co-factors, like chromatin modifying and remodeling enzymes, are certainly required. The contribution of other transcription factors to p53 activity at enhancers (or lack thereof) remains an open question. Recent *in vivo* dissection of p53 enhancer activity implicated the general enhancer-associated AP-1 family member CEBPB as a direct regulator of an enhancer upstream of CDKN1A (68), although whether the requirement for CEBPB is due to regulation of chromatin structure or another activity is unknown. These data support the model whereby

p53 requires the combined activity of other transcription factors at regulatory regions for full transcriptional activation.

Initial observations of p53:nucleosomal DNA binding actually demonstrated higher levels of p53-dependent transcriptional activation than when bound to naked/accessible DNA (52). This pioneer factor activity was confirmed in numerous genomewide and *in vitro* biochemical studies. Of note, not all nucleosome rotational positions permit p53 engagement with its response element which may represent a method of repressing p53 activity at chromatin level (49). p63 appears to share similar nucleosomal binding activities as p53, although detailed biochemical experiments have not yet been undertaken (69, 70). Indeed, our data suggests that p63 binds to many locations that are nucleosome rich, although whether p63 is directly engaging nucleosomal DNA is unclear. The context-specific nucleosomal DNA binding activity of the p53 family, therefore, may be important for both facilitating robust transcriptional activation and for locally regulating p53 family transcription factor activity at chromatin. These data support a model whereby the p53-dependent transcriptome is licensed by the enhancer regulatory abilities of other transcription factors. This model is a particularly attractive avenue for further inquiry and provides a straightforward mechanism for cell type-dependent tumor suppressor and homeostatic activities of p53.

p53 family members have highly conserved DNA binding domains that allow them to engage with highly similar DNA sequences. Therefore, the extent to which p53 family member competition for DNA binding affects their function has been a longstanding question. Initial observations suggested that p63 primarily represses p53 activity in a dominant negative fashion (18, 19). We observed p63-dependent repression of a limited number of p53 targets in MCF10A epithelial cells, supporting the dominant negative model. The specific mechanism by which p63 inhibits p53-dependent transcription requires further investigation, but p63-dependent

HDAC activity and/or H2AZ deposition are attractive models with directly testable hypotheses. However, our results also demonstrated that p63 is required for p53-dependent activation of approximately 40% of epithelial target genes. The precise mechanisms by which p63 supports p53 activity are unclear, but our data demonstrating that p63 likely functions as an enhancer licensing or maintenance factor provides a straightforward possibility. Our model proposes that p63 first establishes a permissive chromatin environment which then allows additional transcription factors, including p53, to bind. This putative mechanism supports both p63-dependent p53 activity and p63-mediated repression. Whereas p63 activity may be required to facilitate a suitable binding environment,  $\Delta N$ -p63 could also repress p53 through local competition for the same binding site. We note that loss of p63 led to substantial gains in p53-dependent H3K27ac enrichment at enhancers, supporting a local inhibition of p53 enhancer activity by p63 through either direct competition or loss of HDAC recruitment. Due to the population-based nature of ChIP-seq, it is uncertain whether p53 and p63 truly compete for binding sites in the same cell, or whether p53 and p63 binding occurs in mutually exclusive cell populations. Therefore, our data confirm p53 and p63 have their previously reported antagonistic relationship and reveal a more broadly cooperative partnership than expected (8, 9).

Our data demonstrate that p63 is required for the stereotypical histone modifications found at p63-bound enhancers in breast basal epithelial cells. Knockdown of p63 in MCF10A cells leads to a site-specific loss of enhancer-associated histone modifications and linked gene expression. These data are consistent with recent work suggesting that p63 activity is critical for epithelial-specific transcriptional programs through control of enhancer identity (42–44). *In vivo*, p63 is required for lineage commitment and self-renewal of basal epithelial cells (38), and p53 family motifs are highly and specifically enriched in epithelial specific enhancers (37). The specific molecular events linking initial p63 DNA binding

to establishment of an active enhancer state and epithelial transcriptional programs are now becoming clearer. p63 interacts with the histone H3K4 monomethylase KMT2D in normal epithelial keratinocytes and reduced KMT2D activity leads to preferential reduction of H3K4me1 at p63-bound enhancers (41). Similarly, inactivation of the BAF chromatin remodeling complex is correlated with reduced chromatin accessibility at p63 binding sites (40).

## EXPERIMENTAL PROCEDURES

### Cell Culture and Treatment

MCF10A mammalian epithelial cells and foreskin fibroblast cells (AG22153, Coriell Institute) were cultured at 37°C in 5% CO<sub>2</sub> in HuMEC Complete media (Gibco, #12752010) and DMEM media (with 10% FBS and 1% Pen/Strep, VWR-0101-0500), respectively. Wild-type and p53-knockout HCT116 colon carcinoma and mouse embryonic fibroblasts were kind gifts of Carol Prives and Jing Huang, respectively. To induce p53 activation, cells were treated with Nutlin-3A (5 μM final, dissolved in DMSO) or DMSO (vehicle control) for 6 hours.

### Western Blotting

Cells were lysed in RIPA buffer (10 mM Tris-HCl (pH 8.0), 1 mM EDTA, 1% Triton X-100, 0.1% sodium deoxycholate, 0.1% SDS and 140 mM NaCl, supplemented freshly with protease inhibitors) and probed with antibodies against p53 (BD Biosciences; BD554293), p63 (Cell Signaling; 13109), TA-p63 (BioLegend; 618901), ΔN-p63 (BioLegend; 619001) and GAPDH (Cell Signaling; 5174). Precision Plus Protein Dual Color Standards protein ladder was used to provide molecular mass markers (Bio-Rad; 1610374).

### RNA-sequencing sample and library preparation

Total mRNA was extracted with E.Z.N.A. Total RNA kit (Omega; R6834-02) and Poly(A)+ RNA was isolated by double selection with poly-dT beads, using 2.5 μg total RNA, which is then

Our data, therefore, place p63 in line with other lineage determination factors that directly act as pioneer transcription factors to license cell type-specific enhancers (71, 72). Further investigation into p63 control of epithelial enhancer identity is required to determine precisely how p63 pioneer activity controls epithelial lineage determination and self-renewal.

followed by first- and second-strand synthesis. Sequencing libraries were prepared using NEXTflex Rapid Illumina DNA-Seq Library Prep Kit (Bioo Scientific). Samples were single-end sequenced on an NextSeq 500. RNA-seq reads were aligned via STAR (73) to Ensembl v.75/hg19. Count tables were generated using STAR-aligned BAM files and HTseq (74). Count tables were then used to call differentially expressed genes using DEseq2 (75).

### Reverse Transcription-Quantitative PCR (RT-qPCR)

Total RNA was extracted as per RNA-sequencing protocol and cDNA was synthesized using 1ug of total RNA as a template and the High-Capacity cDNA Reverse Transcription Kit (Applied Biosystems; 413760). Relative standard qPCR was performed using iTaq Universal SYBR Green Supermix (Bio-Rad; 172-5124) with primers shown in Supplementary Table S8 on an ABI 7900HT instrument.

### Lentivirus production, purification and transduction

Lentiviral shRNAs were produced using HEK293T cells that were seeded in 6 well plates. shRNA sequences are as follows: p53 (GTCCAGATGAAGCTCCCAGAA), p63 (CCGTTTCGTCAGAACACACAT). 1 μg of pLKO plasmid having either scramble shRNA or p53 shRNA or p63 shRNA was combined with 1 μg mix of packaging plasmids (pMD2 and psPAX2) and the mixture was diluted into jetPRIME buffer (Polyplus Transfection; 89129-924) and reagents, following the manufacturer's protocol. Lentivirus containing supernatants were collected at 24 hours and 48 hours post-transfection, and filtered through a 0.45 μm membrane and stored

in aliquots at -80°C. MCF10A or SkFib cells were transfected with lentivirus supplemented with 8 µg/ml polybrene. At 24 hour post-infection with lentivirus, media was replaced with the proper puromycin selection (0.5 µg/ml for MCF10A and 2 µg/ml for SkFib).

### **Chromatin Immunoprecipitation-sequencing (ChIP-seq) sample and library preparation**

Cells were crosslinked at 80% confluence with 1% formaldehyde for 10 min at room temperature. Crosslinking was quenched with 125mM glycine and the resulting pellet was washed twice with cold PBS and lysed as previously described (76). Samples were subjected to sonication with Diagenode Bioruptor Plus for 40 cycles (30 sec on/off at high setting) for shearing chromatin to 150-500 bp average size. Immunoprecipitation reactions for SkFib, MCF10A, and HCT116 cell lines were performed with Diagenode IP-Star Compact Automated System, with the exception of p53 ChIP experiments. Mouse embryonic fibroblast and p53 ChIP-seq were performed as described (29). Antibodies were preconjugated to Protein G beads (Invitrogen) against p63 (Cell Signaling; 13109), H3K4me3 (Active Motif; 39159), H3K4me2 (Millipore; 07-030), H3K27ac (Active Motif, 39133) and p53 monoclonal antibody DO1 (BD Biosciences; BD554293). Immunoprecipitated DNA was reverse-crosslinked at 65°C for 4 hours, eluted, purified using SPRI beads, and used to construct sequencing libraries. Sequencing libraries were prepared using NEBNext Ultra DNA Library Prep Kit for Illumina (New England Biolabs). Prior to sequencing, library quality control was performed with Qubit (Thermo Fisher Scientific), Bioanalyzer (Agilent) and qPCR quantification. All ChIP samples, including input, were single-end sequenced on an NextSeq 500 at the University at Albany Center for Functional Genomics. Uniquely aligned reads (up to one mismatch) were aligned to NCBI37/hg19 using Bowtie2 (77). All ChIP-seq datasets were analyzed for PBC, NSC, and RSC stats as per ENCODE standards (78). Additionally, PBC1, PBC2, and NRF statistics were calculated for p53

and p63 datasets as per ENCODE recommendations for transcription factor ChIP-seq. These quality control (QC) metrics report important information about the molecular complexity of the DNA library (PBC, PBC1, PBC2) and the enrichment of the transcription factor or histone modification (NSC, RSC). These QC metrics combine to give a holistic view of the technical quality of the experiment. All quality control metrics for ChIP-seq datasets can be found in Supplementary Table S9.

### **Chromatin immunoprecipitation and quantitative PCR (ChIP-qPCR)**

MCF10A and skin fibroblasts (both control shRNA or p53 shRNA-expressing) were crosslinked for 10 minutes at room temperature using 1% (final) methanol-free formaldehyde. The crosslinking reaction was quenched with 125mM glycine, washed with ice-cold PBS, and processed for chromatin immunoprecipitation as described above. Samples were then subjected to sonication using the Diagenode Bioruptor Plus for 30 cycles (30 sec on/off at high setting). 1ug of p53 monoclonal antibody DO1 (BD Biosciences; BD554293) or mouse IgG were preconjugated to Protein G beads (Invitrogen), added to sonicated lysate, and then incubated overnight with rotation at 4°C. Samples were then processed as described above for ChIP-sequencing, except that the resulting DNA was used for quantitative PCR reactions to determine p53 genomic occupancy using primer sets listed in Supplementary Table S8.

### **ChIP-seq Peak Calling and Differential Binding Analysis**

Significant regions of transcription factor (p53, p63) and histone modification (H3K4me2, H3K4me3, H3K27ac) enrichment were called using macs v.2.1.0 (33) preserving only peaks with an adjusted P-value < 0.01. All peak calling was performed using sheared chromatin input as the control condition. p53 and p63 motif analysis was performed using p53scan (79) and all macs-derived peaks lacking a p53/p63 consensus motif were removed from further analysis. “High confidence” peaks used in subsequent analyses

represent peaks found in both biological replicates as determined by BEDTools intersectBed (80). A full list of p53/p63 peaks can be found under GEO Accession Number GSE111009. Global transcription factor motif enrichment experiments were performed using the findMotifsGenome.pl script from HOMER (55). An additional approach for calling differential enrichment of p53 ChIP-seq datasets across cell types was performed using DiffBind (81).

#### **Analysis of histone modification enrichment**

Chromatin enrichment analyses were performed using the annotatePeaks.pl script of HOMER. Read-depth-scaled chromatin tag enrichment within a specified window was input-normalized (target – input) and then further scaled to total genomewide enrichment of peaks for that histone modification. Analyses of H3K4me3 enrichment and gene expression from mouse embryonic fibroblasts was previously described (GSE59176) (82).

#### **Computational Analysis and Plotting**

Peak file intersections were performed using the intersectBed package of BedTools (80), scoring positive intersections as those with at least 1bp of overlap (-f 1E-9). The original peak file (-a) was reported only once (-u) if any intersection exists with the query file (-b). The closestBed package of BedTools was used to measure distances between features with the distance reported using the -d option. Figures were generated using Graphpad Prism or Datagraph. Bigwig (bw) files were generated with the bamCoverage package of deepTools v.2.5.4 (83) with a bin size of 1 (--binSize 1) and read extension (--extendReads 300). Heatmaps were then generated using bigwig files for a +/- 1000bp region from the p53/p63 peak center using the computeMatrix (reference-point, -a 1000, -b

1000, --binSize 10) and plotHeatmap functions. Genome browser tracks (bedGraph) were generated using the makeUCSCfile.pl package of HOMER (55). K-means clustering was performed using cluster 3.0 for Mac.

#### **Statistical Testing**

Statistical testing was performed using Graphpad Prism (v. 7) or using the built-in stats package in R (v.3.4.0).

#### **ChromHMM chromatin state and DNase hypersensitive site (DHS) enrichment analysis**

ChromHMM analysis (84) was performed using the 25 state model ([http://egg2.wustl.edu/roadmap/web\\_portal/](http://egg2.wustl.edu/roadmap/web_portal/)), with at least 50% of the p53/p63 motif required to overlap a single chromatin enrichment term (closestBed -a p53.file -b ChromHMM.file -d -f 0.51). The 25 chromatin state models for ChromHMM terms were combined into 4 regulatory terms: enhancer, repressive, quiescent, or transcription. A full list of p53, p63, and p53/p63 binding site regulatory region inferences across the 127 cell types of the ChromHMM analysis can be found in Supplementary Table S10. DHS data were downloaded from <http://hgdownload.cse.ucsc.edu/goldenpath/hg19/encodeDCC/wgEncodeRegDnaseClustered/>. Intersection of p53/p63 peaks with DHS data was performed using the closestBed package of BedTools, with 100% of the p53/p63 motif required to overlap the DHS (-f 1). Data are grouped by epithelial or non-epithelial cell types.

#### **Accession Numbers and Data Availability**

All new raw data associated with this study are deposited at NCBI Gene Expression Omnibus under accession number GSE111009.

#### **CONFLICT OF INTEREST**

The authors declare that they have no conflicts of interest with the contents of this article. The content is solely the responsibility of the authors and does not necessarily represent the official views of the National Institutes of Health.

## **ACKNOWLEDGEMENTS**

We are grateful to Allison Catizone and Enrique Lin Shiao for feedback on this manuscript. We thank Jason Herschkowitz, Carol Prives, and Jing Huang for the MCF10A, HCT116 p53 KO, and MEF p53 KO cell lines, respectively. We also thank the University at Albany Center for Functional Genomics for sequencing support. This work is supported by start-up funds from the State University of New York at Albany and NIH R15 GM128049.

## REFERENCES

1. Levriero, M., Laurenzi, V. D., Costanzo, A., Gong, J., Wang, J. Y., and Melino, G. (2000) The p53/p63/p73 family of transcription factors: overlapping and distinct functions. *J Cell Sci.* **113**, 1661–1670
2. Kastenhuber, E. R., and Lowe, S. W. (2017) Putting p53 in Context. *Cell.* **170**, 1062–1078
3. Andrysiak, Z., Galbraith, M. D., Guarnieri, A. L., Zaccara, S., Sullivan, K. D., Pandey, A., MacBeth, M., Inga, A., and Espinosa, J. M. (2017) Identification of a core TP53 transcriptional program with highly distributed tumor suppressive activity. *Genome Res.* **27**, 1645–1657
4. Li, T., Kon, N., Jiang, L., Tan, M., Ludwig, T., Zhao, Y., Baer, R., and Gu, W. (2012) Tumor suppression in the absence of p53-mediated cell-cycle arrest, apoptosis, and senescence. *Cell.* **149**, 1269–83
5. Zhu, J., Dou, Z., Sammons, M. A., Levine, A. J., and Berger, S. L. (2016) Lysine methylation represses p53 activity in teratocarcinoma cancer cells. *Proc. Natl. Acad. Sci. U. S. A.* **113**, 9822–9827
6. Ciriello, G., Miller, M. L., Aksoy, B. A., Senbabaooglu, Y., Schultz, N., and Sander, C. (2013) Emerging landscape of oncogenic signatures across human cancers. *Nat Genet.* **45**, 1127–33
7. Kandoth, C., McLellan, M. D., Vandin, F., Ye, K., Niu, B., Lu, C., Xie, M., Zhang, Q., McMichael, J. F., Wyczalkowski, M. A., Leiserson, M. D., Miller, C. A., Welch, J. S., Walter, M. J., Wendl, M. C., Ley, T. J., Wilson, R. K., Raphael, B. J., and Ding, L. (2013) Mutational landscape and significance across 12 major cancer types. *Nature.* **502**, 333–9
8. Flores, E. R., Tsai, K. Y., Crowley, D., Sengupta, S., Yang, A., McKeon, F., and Jacks, T. (2002) p63 and p73 are required for p53-dependent apoptosis in response to DNA damage. *Nature.* **416**, 560–564
9. Botchkarev, V. A., and Flores, E. R. (2014) p53/p63/p73 in the epidermis in health and disease. *Cold Spring Harb Perspect Med.* 10.1101/cshperspect.a015248
10. DeYoung, M. P., and Ellisen, L. W. (2007) p63 and p73 in human cancer: defining the network. *Oncogene.* **26**, 5169–5183
11. Melino, G., Memmi, E. M., Pelicci, P. G., and Bernassola, F. (2015) Maintaining epithelial stemness with p63. *Sci Signal.* **8**, re9
12. Fakhouri, W. D., Rahimov, F., Attanasio, C., Kouwenhoven, E. N., Ferreira De Lima, R. L., Felix, T. M., Nitschke, L., Huver, D., Barrons, J., Kousa, Y. A., Leslie, E., Pennacchio, L. A., Van Bokhoven, H., Visel, A., Zhou, H., Murray, J. C., and Schutte, B. C. (2014) An etiologic regulatory mutation in IRF6 with loss- and gain-of-function effects. *Hum Mol Genet.* **23**, 2711–20
13. Brunner, H. G., Hamel, B. C., and Van Bokhoven, H. (2002) The p63 gene in EEC and other syndromes. *J Med Genet.* **39**, 377–81
14. Moll, U. M., Erster, S., and Zaika, A. (2001) p53, p63 and p73—solos, alliances and feuds among family members. *Biochim. Biophys. Acta.* **1552**, 47–59
15. Billant, O., Leon, A., Le Guellec, S., Friocourt, G., Blondel, M., and Voisset, C. (2016) The dominant-negative interplay between p53, p63 and p73: A family affair. *Oncotarget.* **7**, 69549–69564
16. McDade, S. S., Patel, D., Moran, M., Campbell, J., Fenwick, K., Kozarewa, I., Orr, N. J., Lord, C. J., Ashworth, A. A., and McCance, D. J. (2014) Genome-wide characterization reveals complex interplay between TP53 and TP63 in response to genotoxic stress. *Nucleic Acids Res.* **42**, 6270–85

17. Yang, A., Zhu, Z., Kapranov, P., McKeon, F., Church, G. M., Gingeras, T. R., and Struhl, K. (2006) Relationships between p63 Binding, DNA Sequence, Transcription Activity, and Biological Function in Human Cells. *Mol. Cell.* **24**, 593–602
18. Yang, A., Kaghad, M., Wang, Y., Gillett, E., Fleming, M. D., Dötsch, V., Andrews, N. C., Caput, D., and McKeon, F. (1998) p63, a p53 Homolog at 3q27–29, Encodes Multiple Products with Transactivating, Death-Inducing, and Dominant-Negative Activities. *Mol. Cell.* **2**, 305–316
19. Mundt, H. M., Stremmel, W., Melino, G., Krammer, P. H., Schilling, T., and Müller, M. (2010) Dominant negative (DeltaN) p63alpha induces drug resistance in hepatocellular carcinoma by interference with apoptosis signaling pathways. *Biochem. Biophys. Res. Commun.* **396**, 335–341
20. Gallant-Behm, C. L., and Espinosa, J. M. (2013) DeltaNp63alpha utilizes multiple mechanisms to repress transcription in squamous cell carcinoma cells. *Cell Cycle.* **12**, 409–16
21. Gallant-Behm, C. L., Ramsey, M. R., Bensard, C. L., Nojek, I., Tran, J., Liu, M., Ellisen, L. W., and Espinosa, J. M. (2012) ΔNp63α represses anti-proliferative genes via H2A.Z deposition. *Genes Dev.* **26**, 2325–2336
22. Ramsey, M. R., He, L., Forster, N., Ory, B., and Ellisen, L. W. (2011) Physical association of HDAC1 and HDAC2 with p63 mediates transcriptional repression and tumor maintenance in squamous cell carcinoma. *Cancer Res.* **71**, 4373–4379
23. LeBoeuf, M., Terrell, A., Trivedi, S., Sinha, S., Epstein, J. A., Olson, E. N., Morrisey, E. E., and Millar, S. E. (2010) Hdac1 and Hdac2 act redundantly to control p63 and p53 functions in epidermal progenitor cells. *Dev. Cell.* **19**, 807–818
24. Saladi, S. V., Ross, K., Karaayvaz, M., Tata, P. R., Mou, H., Rajagopal, J., Ramaswamy, S., and Ellisen, L. W. (2017) ACTL6A Is Co-Amplified with p63 in Squamous Cell Carcinoma to Drive YAP Activation, Regenerative Proliferation, and Poor Prognosis. *Cancer Cell.* **31**, 35–49
25. Verfaillie, A., Svetlichnyy, D., Imrichova, H., Davie, K., Fiers, M., Kalender Atak, Z., Hulselmans, G., Christiaens, V., and Aerts, S. (2016) Multiplex enhancer-reporter assays uncover unsophisticated TP53 enhancer logic. *Genome Res.* **26**, 882–895
26. Younger, S. T., and Rinn, J. L. (2017) p53 regulates enhancer accessibility and activity in response to DNA damage. *Nucleic Acids Res.* **45**, 9889–9900
27. Nguyen, T.-A. T., Grimm, S. A., Bushel, P. R., Li, J., Li, Y., Bennett, B. D., Lavender, C. A., Ward, J. M., Fargo, D. C., Anderson, C. W., Li, L., Resnick, M. A., and Menendez, D. (2018) Revealing a human p53 universe. *Nucleic Acids Res.* **10.1093/nar/gky720**
28. Hafner, A., Lahav, G., and Stewart-Ornstein, J. (2017) Stereotyped p53 binding tuned by chromatin accessibility. *bioRxiv*
29. Sammons, M. A., Zhu, J., Drake, A. M., and Berger, S. L. (2015) TP53 engagement with the genome occurs in distinct local chromatin environments via pioneer factor activity. *Genome Res.* **25**, 179–88
30. Vassilev, L. T., Vu, B. T., Graves, B., Carvajal, D., Podlaski, F., Filipovic, Z., Kong, N., Kammlott, U., Lukacs, C., Klein, C., Fotouhi, N., and Liu, E. A. (2004) In vivo activation of the p53 pathway by small-molecule antagonists of MDM2. *Science.* **303**, 844–848
31. Allen, M. A., Andrysik, Z., Dengler, V. L., Mellert, H. S., Guarnieri, A., Freeman, J. A., Sullivan, K. D., Galbraith, M. D., Luo, X., Kraus, W. L., Dowell, R. D., and Espinosa, J. M. (2014) Global analysis of p53-regulated transcription identifies its direct targets and unexpected regulatory mechanisms. *Elife.* **3**, e02200
32. Fischer, M. (2017) Census and evaluation of p53 target genes. *Oncogene.* **36**, 3943–3956
33. Zhang, Y., Liu, T., Meyer, C. A., Eeckhoute, J., Johnson, D. S., Bernstein, B. E., Nusbaum, C., Myers, R. M., Brown, M., Li, W., and Liu, X. S. (2008) Model-based analysis of ChIP-Seq (MACS). *Genome Biol.* **9**, R137

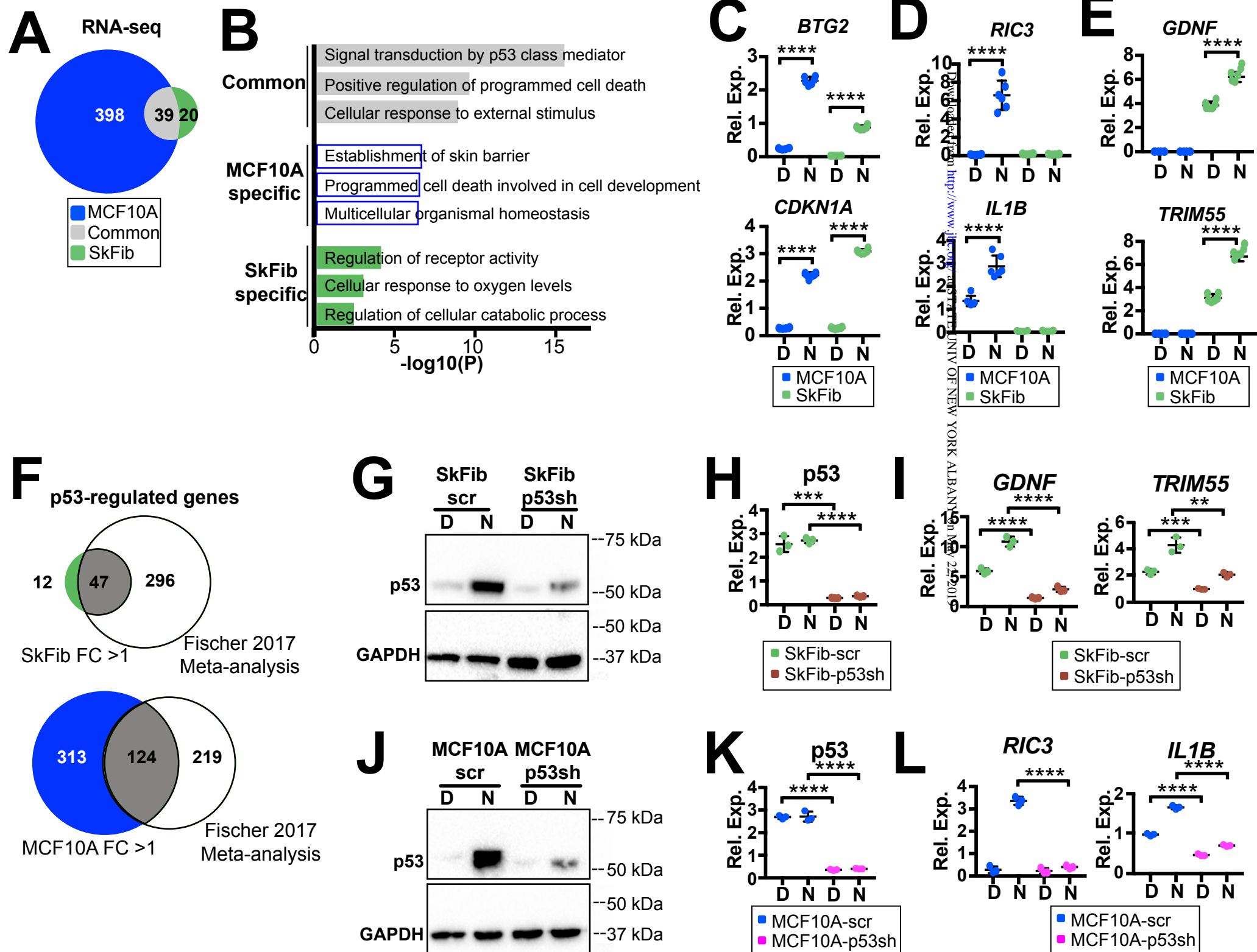
34. Sullivan, K. D., Galbraith, M. D., Andrysik, Z., and Espinosa, J. M. (2018) Mechanisms of transcriptional regulation by p53. *Cell Death Differ.* **25**, 133–143
35. Calo, E., and Wysocka, J. (2013) Modification of Enhancer Chromatin: What, How, and Why? *Mol. Cell.* **49**, 825–837
36. Heinz, S., Romanoski, C. E., Benner, C., and Glass, C. K. (2015) The selection and function of cell type-specific enhancers. *Nat. Rev. Mol. Cell Biol.* **16**, 144–154
37. The FANTOM Consortium, Andersson, R., Gebhard, C., Miguel-Escalada, I., Hoof, I., Bornholdt, J., Boyd, M., Chen, Y., Zhao, X., Schmidl, C., Suzuki, T., Ntini, E., Arner, E., Valen, E., Li, K., Schwarzbacher, L., Glatz, D., Raithel, J., Lilje, B., Rapin, N., Bagger, F. O., Jørgensen, M., Andersen, P. R., Bertin, N., Rackham, O., Burroughs, A. M., Baillie, J. K., Ishizu, Y., Shimizu, Y., Furuhata, E., Maeda, S., Negishi, Y., Mungall, C. J., Meehan, T. F., Lassmann, T., Itoh, M., Kawaji, H., Kondo, N., Kawai, J., Lennartsson, A., Daub, C. O., Heutink, P., Hume, D. A., Jensen, T. H., Suzuki, H., Hayashizaki, Y., Müller, F., Forrest, A. R. R., Carninci, P., Rehli, M., and Sandelin, A. (2014) An atlas of active enhancers across human cell types and tissues. *Nature.* **507**, 455–461
38. Yang, A., Schweitzer, R., Sun, D., Kaghad, M., Walker, N., Bronson, R. T., Tabin, C., Sharpe, A., Caput, D., Crum, C., and McKeon, F. (1999) p63 is essential for regenerative proliferation in limb, craniofacial and epithelial development. *Nature.* **398**, 714–8
39. Kouwenhoven, E. N., Oti, M., Niehues, H., van Heeringen, S. J., Schalkwijk, J., Stunnenberg, H. G., van Bokhoven, H., and Zhou, H. (2015) Transcription factor p63 bookmarks and regulates dynamic enhancers during epidermal differentiation. *EMBO Rep.* **16**, 863–78
40. Bao, X., Rubin, A. J., Qu, K., Zhang, J., Giresi, P. G., Chang, H. Y., and Khavari, P. A. (2015) A novel ATAC-seq approach reveals lineage-specific reinforcement of the open chromatin landscape via cooperation between BAF and p63. *Genome Biol.* **16**, 284
41. Lin-Shiao, E., Lan, Y., Coradin, M., Anderson, A., Donahue, G., Simpson, C. L., Sen, P., Saffie, R., Busino, L., Garcia, B. A., Berger, S. L., and Capell, B. C. (2018) KMT2D regulates p63 target enhancers to coordinate epithelial homeostasis. *Genes Dev.* **32**, 181–193
42. Qu, J., Tanis, S. E. J., Smits, J. P. H., Kouwenhoven, E. N., Oti, M., Bogaard, E. H. van den, Logie, C., Stunnenberg, H. G., Bokhoven, H. van, Mulder, K. W., and Zhou, H. (2018) Mutant p63 Affects Epidermal Cell Identity through Rewiring the Enhancer Landscape. *Cell Rep.* **25**, 3490–3503.e4
43. Pattison, J. M., Melo, S. P., Piekos, S. N., Torkelson, J. L., Bashkirova, E., Mumbach, M. R., Rajasingh, C., Zhen, H. H., Li, L., Liaw, E., Alber, D., Rubin, A. J., Shankar, G., Bao, X., Chang, H. Y., Khavari, P. A., and Oro, A. E. (2018) Retinoic acid and BMP4 cooperate with p63 to alter chromatin dynamics during surface epithelial commitment. *Nat. Genet.* **50**, 1658
44. Li, L., Wang, Y., Torkelson, J. L., Shankar, G., Pattison, J. M., Zhen, H. H., Fang, F., Duren, Z., Xin, J., Gaddam, S., Melo, S. P., Piekos, S. N., Li, J., Liaw, E. J., Chen, L., Li, R., Wernig, M., Wong, W. H., Chang, H. Y., and Oro, A. E. (2019) TFAP2C- and p63-Dependent Networks Sequentially Rearrange Chromatin Landscapes to Drive Human Epidermal Lineage Commitment. *Cell Stem Cell.* 10.1016/j.stem.2018.12.012
45. Marshall, C. B., Mays, D. J., Beeler, J. S., Rosenbluth, J. M., Boyd, K. L., Santos Guasch, G. L., Shaver, T. M., Tang, L. J., Liu, Q., Shyr, Y., Venters, B. J., Magnuson, M. A., and Pietenpol, J. A. (2016) p73 Is Required for Multiciliogenesis and Regulates the Foxj1-Associated Gene Network. *Cell Rep.* **14**, 2289–2300
46. Nemajerova, A., Kramer, D., Siller, S. S., Herr, C., Shomroni, O., Pena, T., Gallinas Suazo, C., Glaser, K., Wildung, M., Steffen, H., Sriraman, A., Oberle, F., Wienken, M., Hennion, M., Vidal, R., Royen, B., Alevra, M., Schild, D., Bals, R., Dönitz, J., Riedel, D., Bonn, S., Takemaru, K.-I.,

- Moll, U. M., and Lizé, M. (2016) TAp73 is a central transcriptional regulator of airway multiciliogenesis. *Genes Dev.* **30**, 1300–1312
47. Koster, M. I., Kim, S., Mills, A. A., DeMayo, F. J., and Roop, D. R. (2004) p63 is the molecular switch for initiation of an epithelial stratification program. *Genes Dev.* **18**, 126–131
48. Carroll, D. K., Carroll, J. S., Leong, C.-O., Cheng, F., Brown, M., Mills, A. A., Brugge, J. S., and Ellisen, L. W. (2006) p63 regulates an adhesion programme and cell survival in epithelial cells. *Nat. Cell Biol.* **8**, 551
49. Cui, F., and Zhurkin, V. B. (2014) Rotational positioning of nucleosomes facilitates selective binding of p53 to response elements associated with cell cycle arrest. *Nucleic Acids Res.* **42**, 836–47
50. Lin-Shiao, E., Lan, Y., Welzenbach, J., Alexander, K. A., Zhang, Z., Knapp, M., Mangold, E., Sammons, M., Ludwig, K. U., and Berger, S. L. (2019) p63 establishes epithelial enhancers at critical craniofacial development genes. *Sci. Adv.* **5**, eaaw0946
51. Nili, E. L., Field, Y., Lubling, Y., Widom, J., Oren, M., and Segal, E. (2010) p53 binds preferentially to genomic regions with high DNA-encoded nucleosome occupancy. *Genome Res.* **20**, 1361–1368
52. Espinosa, J. M., Verdun, R. E., and Emerson, B. M. (2003) p53 functions through stress- and promoter-specific recruitment of transcription initiation components before and after DNA damage. *Mol. Cell.* **12**, 1015–1027
53. Reiter, F., Wienerroither, S., and Stark, A. (2017) Combinatorial function of transcription factors and cofactors. *Curr. Opin. Genet. Dev.* **43**, 73–81
54. Shlyueva, D., Stampfel, G., and Stark, A. (2014) Transcriptional enhancers: from properties to genome-wide predictions. *Nat. Rev. Genet.* **15**, 272–286
55. Heinz, S., Benner, C., Spann, N., Bertolino, E., Lin, Y. C., Laslo, P., Cheng, J. X., Murre, C., Singh, H., and Glass, C. K. (2010) Simple combinations of lineage-determining transcription factors prime cis-regulatory elements required for macrophage and B cell identities. *Mol. Cell.* **38**, 576–589
56. Biddie, S. C., John, S., Sabo, P. J., Thurman, R. E., Johnson, T. A., Schiltz, R. L., Miranda, T. B., Sung, M.-H., Trump, S., Lightman, S. L., Vinson, C., Stamatoyannopoulos, J. A., and Hager, G. L. (2011) Transcription factor AP1 potentiates chromatin accessibility and glucocorticoid receptor binding. *Mol. Cell.* **43**, 145–155
57. Boxer, L. D., Barajas, B., Tao, S., Zhang, J., and Khavari, P. A. (2014) ZNF750 interacts with KLF4 and RCOR1, KDM1A, and CTBP1/2 chromatin regulators to repress epidermal progenitor genes and induce differentiation genes. *Genes Dev.* **28**, 2013–2026
58. Sen, G. L., Boxer, L. D., Webster, D. E., Bussat, R. T., Qu, K., Zarnegar, B. J., Johnston, D., Siprashvili, Z., and Khavari, P. A. (2012) ZNF750 is a p63 target gene that induces KLF4 to drive terminal epidermal differentiation. *Dev. Cell.* **22**, 669–677
59. Rotter, V., Schwartz, D., Almon, E., Goldfinger, N., Kapon, A., Meshorer, A., Donehower, L. A., and Levine, A. J. (1993) Mice with reduced levels of p53 protein exhibit the testicular giant-cell degenerative syndrome. *Proc. Natl. Acad. Sci. U. S. A.* **90**, 9075–9079
60. Armstrong, J. F., Kaufman, M. H., Harrison, D. J., and Clarke, A. R. (1995) High-frequency developmental abnormalities in p53-deficient mice. *Curr. Biol. CB.* **5**, 931–936
61. Sah, V. P., Attardi, L. D., Mulligan, G. J., Williams, B. O., Bronson, R. T., and Jacks, T. (1995) A subset of p53-deficient embryos exhibit exencephaly. *Nat. Genet.* **10**, 175–180
62. Powell, E., Piwnica-Worms, D., and Piwnica-Worms, H. (2014) Contribution of p53 to metastasis. *Cancer Discov.* **4**, 405–414
63. Chang, C.-J., Chao, C.-H., Xia, W., Yang, J.-Y., Xiong, Y., Li, C.-W., Yu, W.-H., Rehman, S. K., Hsu, J. L., Lee, H.-H., Liu, M., Chen, C.-T., Yu, D., and Hung, M.-C. (2011) p53 regulates

- epithelial–mesenchymal transition and stem cell properties through modulating miRNAs. *Nat. Cell Biol.* **13**, 317–323
64. Hermeking, H., Lengauer, C., Polyak, K., He, T.-C., Zhang, L., Thiagalingam, S., Kinzler, K. W., and Vogelstein, B. (1997) 14-3-3 $\sigma$  Is a p53-Regulated Inhibitor of G2/M Progression. *Mol. Cell.* **1**, 3–11
  65. Mungamuri, S. K., Benson, E. K., Wang, S., Gu, W., Lee, S. W., and Aaronson, S. A. (2012) p53-mediated heterochromatin reorganization regulates its cell fate decisions. *Nat. Struct. Mol. Biol.* **19**, 478–484
  66. París, R., Henry, R. E., Stephens, S. J., McBryde, M., and Espinosa, J. M. (2008) Multiple p53-independent gene silencing mechanisms define the cellular response to p53 activation. *Cell Cycle* **7**, 2427–2433
  67. Yu, X., and Buck, M. J. (2019) Defining TP53 pioneering capabilities with competitive nucleosome binding assays. *Genome Res.* **29**, 107–115
  68. Korkmaz, G., Lopes, R., Ugalde, A. P., Nevedomskaya, E., Han, R., Myacheva, K., Zwart, W., Elkon, R., and Agami, R. (2016) Functional genetic screens for enhancer elements in the human genome using CRISPR-Cas9. *Nat. Biotechnol.* **34**, 192–198
  69. Sethi, I., Gluck, C., Zhou, H., Buck, M. J., and Sinha, S. (2017) Evolutionary re-wiring of p63 and the epigenomic regulatory landscape in keratinocytes and its potential implications on species-specific gene expression and phenotypes. *Nucleic Acids Res.* **45**, 8208–8224
  70. Sethi, I., Sinha, S., and Buck, M. J. (2014) Role of chromatin and transcriptional co-regulators in mediating p63-genome interactions in keratinocytes. *BMC Genomics* **15**, 1042
  71. Zaret, K. S., and Carroll, J. S. (2011) Pioneer transcription factors: establishing competence for gene expression. *Genes Dev.* **25**, 2227–41
  72. Zaret, K. S., and Mango, S. E. (2016) Pioneer transcription factors, chromatin dynamics, and cell fate control. *Curr Opin Genet Dev.* **37**, 76–81
  73. Dobin, A., Davis, C. A., Schlesinger, F., Drenkow, J., Zaleski, C., Jha, S., Batut, P., Chaisson, M., and Gingeras, T. R. (2013) STAR: ultrafast universal RNA-seq aligner. *Bioinforma. Oxf. Engl.* **29**, 15–21
  74. Anders, S., Pyl, P. T., and Huber, W. (2015) HTSeq--a Python framework to work with high-throughput sequencing data. *Bioinforma. Oxf. Engl.* **31**, 166–169
  75. Love, M. I., Huber, W., and Anders, S. (2014) Moderated estimation of fold change and dispersion for RNA-seq data with DESeq2. *Genome Biol.* **15**, 550
  76. Lee, T. I., Johnstone, S. E., and Young, R. A. (2006) Chromatin immunoprecipitation and microarray-based analysis of protein location. *Nat. Protoc.* **1**, 729–748
  77. Langmead, B., and Salzberg, S. L. (2012) Fast gapped-read alignment with Bowtie 2. *Nat. Methods* **9**, 357–359
  78. Landt, S. G., Marinov, G. K., Kundaje, A., Kheradpour, P., Pauli, F., Batzoglou, S., Bernstein, B. E., Bickel, P., Brown, J. B., Cayting, P., Chen, Y., DeSalvo, G., Epstein, C., Fisher-Aylor, K. I., Euskirchen, G., Gerstein, M., Gertz, J., Hartemink, A. J., Hoffman, M. M., Iyer, V. R., Jung, Y. L., Karmakar, S., Kellis, M., Kharchenko, P. V., Li, Q., Liu, T., Liu, X. S., Ma, L., Milosavljevic, A., Myers, R. M., Park, P. J., Pazin, M. J., Perry, M. D., Raha, D., Reddy, T. E., Rozowsky, J., Shores, N., Sidow, A., Slattery, M., Stamatoyannopoulos, J. A., Tolstorukov, M. Y., White, K. P., Xi, S., Farnham, P. J., Lieb, J. D., Wold, B. J., and Snyder, M. (2012) ChIP-seq guidelines and practices of the ENCODE and modENCODE consortia. *Genome Res.* **22**, 1813–1831
  79. Smeenk, L., van Heeringen, S. J., Koeppel, M., van Driel, M. A., Bartels, S. J., Akkers, R. C., Denissov, S., Stunnenberg, H. G., and Lohrum, M. (2008) Characterization of genome-wide p53-binding sites upon stress response. *Nucleic Acids Res.* **36**, 3639–54

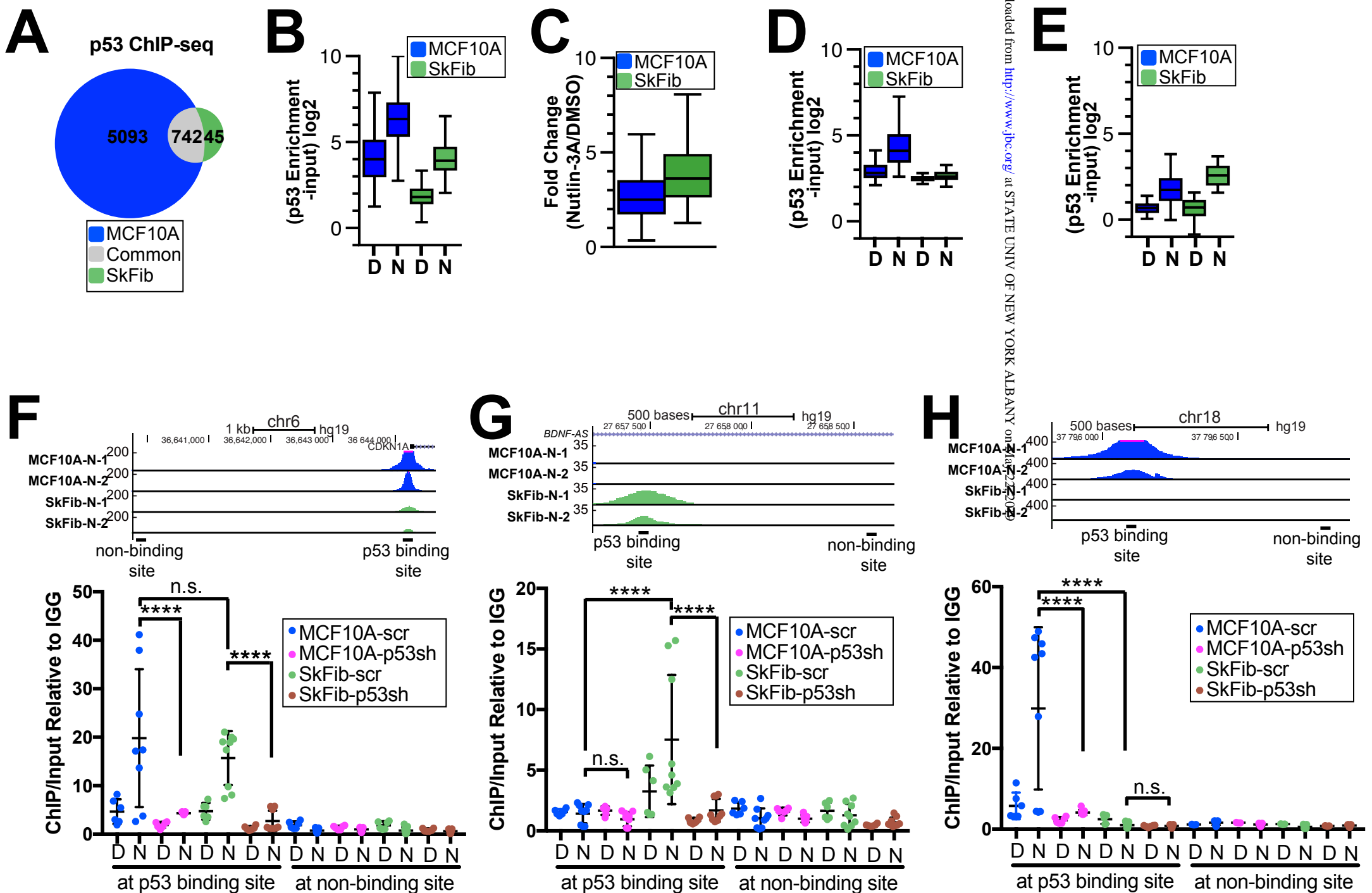
80. Quinlan, A. R., and Hall, I. M. (2010) BEDTools: a flexible suite of utilities for comparing genomic features. *Bioinformatics*. **26**, 841–842
81. Ross-Innes, C. S., Stark, R., Teschendorff, A. E., Holmes, K. A., Ali, H. R., Dunning, M. J., Brown, G. D., Gojis, O., Ellis, I. O., Green, A. R., Ali, S., Chin, S.-F., Palmieri, C., Caldas, C., and Carroll, J. S. (2012) Differential oestrogen receptor binding is associated with clinical outcome in breast cancer. *Nature*. **481**, 389–393
82. Zhu, J., Sammons, M. A., Donahue, G., Dou, Z., Vedadi, M., Getlik, M., Barsyte-Lovejoy, D., Al-awar, R., Katona, B. W., Shilatifard, A., Huang, J., Hua, X., Arrowsmith, C. H., and Berger, S. L. (2015) Gain-of-function p53 mutants co-opt chromatin pathways to drive cancer growth. *Nature*. **525**, 206–211
83. Ramírez, F., Ryan, D. P., Grüning, B., Bhardwaj, V., Kilpert, F., Richter, A. S., Heyne, S., Dündar, F., and Manke, T. (2016) deepTools2: a next generation web server for deep-sequencing data analysis. *Nucleic Acids Res.* **44**, W160–W165
84. Ernst, J., and Kellis, M. (2012) ChromHMM: automating chromatin-state discovery and characterization. *Nat. Methods*. **9**, 215–216
85. Kenzelmann Broz, D., Spano Mello, S., Bieging, K. T., Jiang, D., Dusek, R. L., Brady, C. A., Sidow, A., and Attardi, L. D. (2013) Global genomic profiling reveals an extensive p53-regulated autophagy program contributing to key p53 responses. *Genes Dev.* **27**, 1016–31

Figure 1



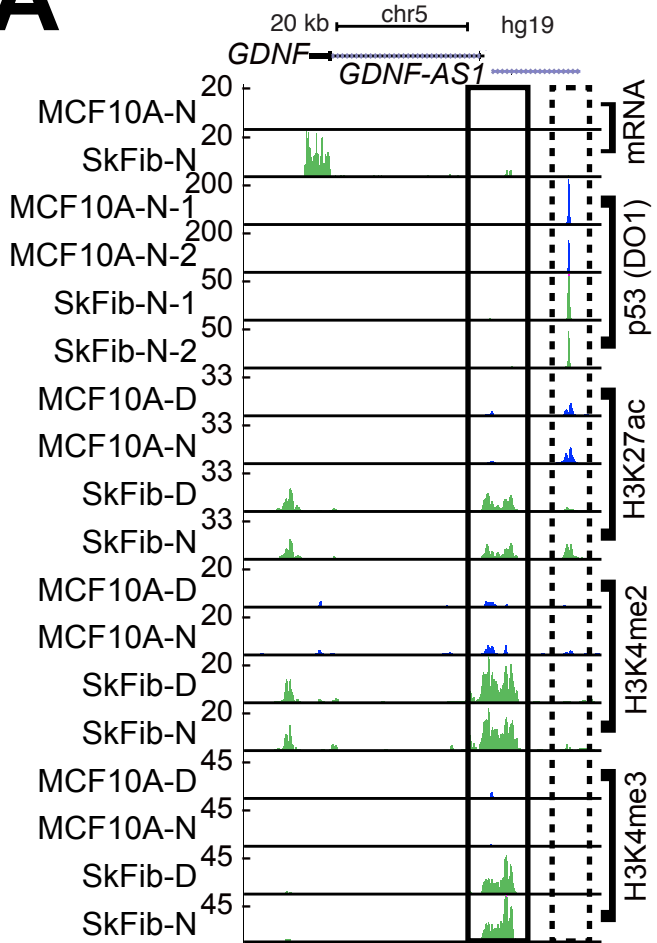
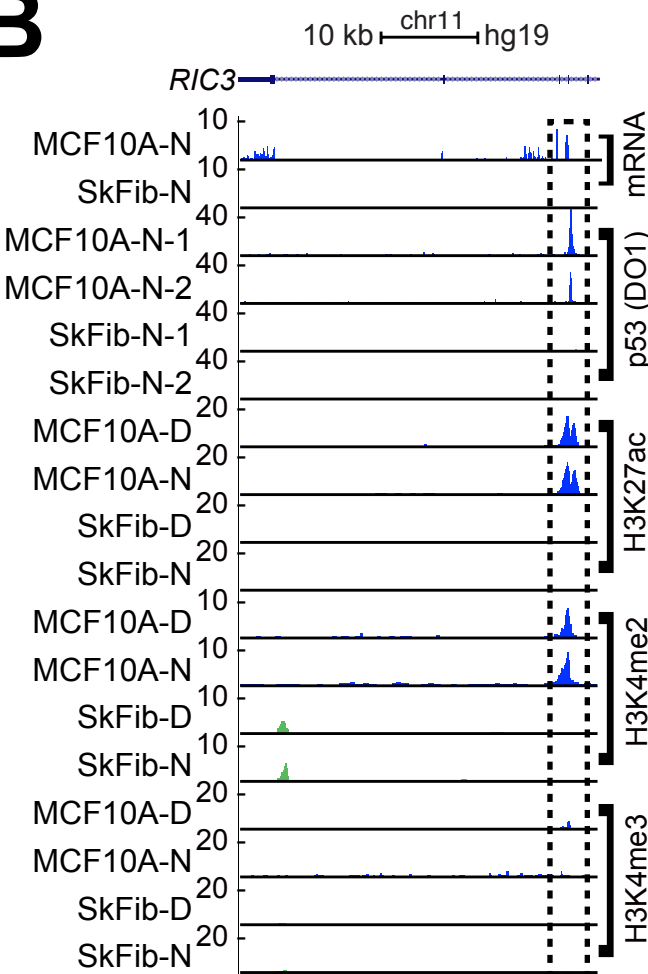
**Figure 1.** **(A)** Venn diagram indicating differentially upregulated genes (Nutlin-3A/DMSO, fold change  $\geq 2$ , adjusted  $p < 0.05$ ) in MCF10A or SkFib cells. **(B)** Gene ontology analysis of differentially expressed genes from MCF10A and SkFib cells showing upregulated genes for top three significant biological processes. **(C-D)** qRT-PCR validation of two representative **(C)** common, **(D)** MCF10A-, and **(E)** SkFib-specific Nutlin-3A-induced targets. Target gene expression is normalized to GAPDH (Relative expression: Rel. Exp.) and data represent technical replicates from three independent biological replicates. Error bars represent SEM with  $p$  values calculated by Student's t-test, \*\*\*\* $p < 0.0001$ . **(F)** Intersection between SkFib (top) or MCF10A (bottom) p53 targets identified in this work compared to the meta-analysis of p53 targets identified in at least 3 independent experiments (Fischer, M 2017). **(G)** Immunoblotting for p53 expression at 6 hours of DMSO (D) or Nutlin-3A (N) treatment in SkFib cells stably expressing shRNA against p53 (p53sh) or a non-targeting control shRNA (scr). **(H)** qRT-PCR analysis of p53 expression at 6 hours of DMSO (D) or Nutlin-3A (N) treatment in SkFib cells stably expressing shRNA against p53 (p53sh) or a non-targeting control shRNA (scr). p53 expression is normalized to GAPDH expression (Relative expression). Error bars represent SEM; \*\*\*\* $p < 0.0001$  and \*\*\* $p < 0.001$ , calculated by Student's t-test. **(I)** qRT-PCR analysis of SkFib-specific gene targets, *GDNF* and *TRIM55*, in SkFib cells stably expressing an shRNA to p53 (p53sh) or a non-targeting control shRNA (scr). Gene expression is normalized to GAPDH expression. Error bars represent SEM; \*\*\*\* $p < 0.0001$ , \*\*\* $p < 0.001$  and \*\* $p < 0.01$ , calculated by Student's t-test. **(J)** Immunoblotting for p53 expression at 6 hours of DMSO (D) or Nutlin-3A (N) treatment in response to p53 knockdown in MCF10A cells stably expressing shRNA against p53 or a non-targeting control shRNA (scr). **(K)** qRT-PCR analysis of p53 expression at 6 hours of DMSO (D) or Nutlin-3A (N) treatment in response to p53 knockdown in MCF10A cells stably expressing shRNA against p53 or a non-targeting control shRNA (scr). p53 RNA expression is normalized to GAPDH expression. Error bars represent SEM; \*\*\*\* $p < 0.0001$ , calculated by Student's t-test. **(L)** qRT-PCR analysis of MCF10A-specific Nutlin-3A-induced genes, *R/C3* and *IL1B*, in MCF10A cells stably expressing an shRNA to p53 (p53 sh) or a non-targeting control shRNA (scr). Expression is normalized to GAPDH expression. Error bars represent SEM; \*\*\*\* $p < 0.0001$ , calculated by Student's t-test.

Figure 2



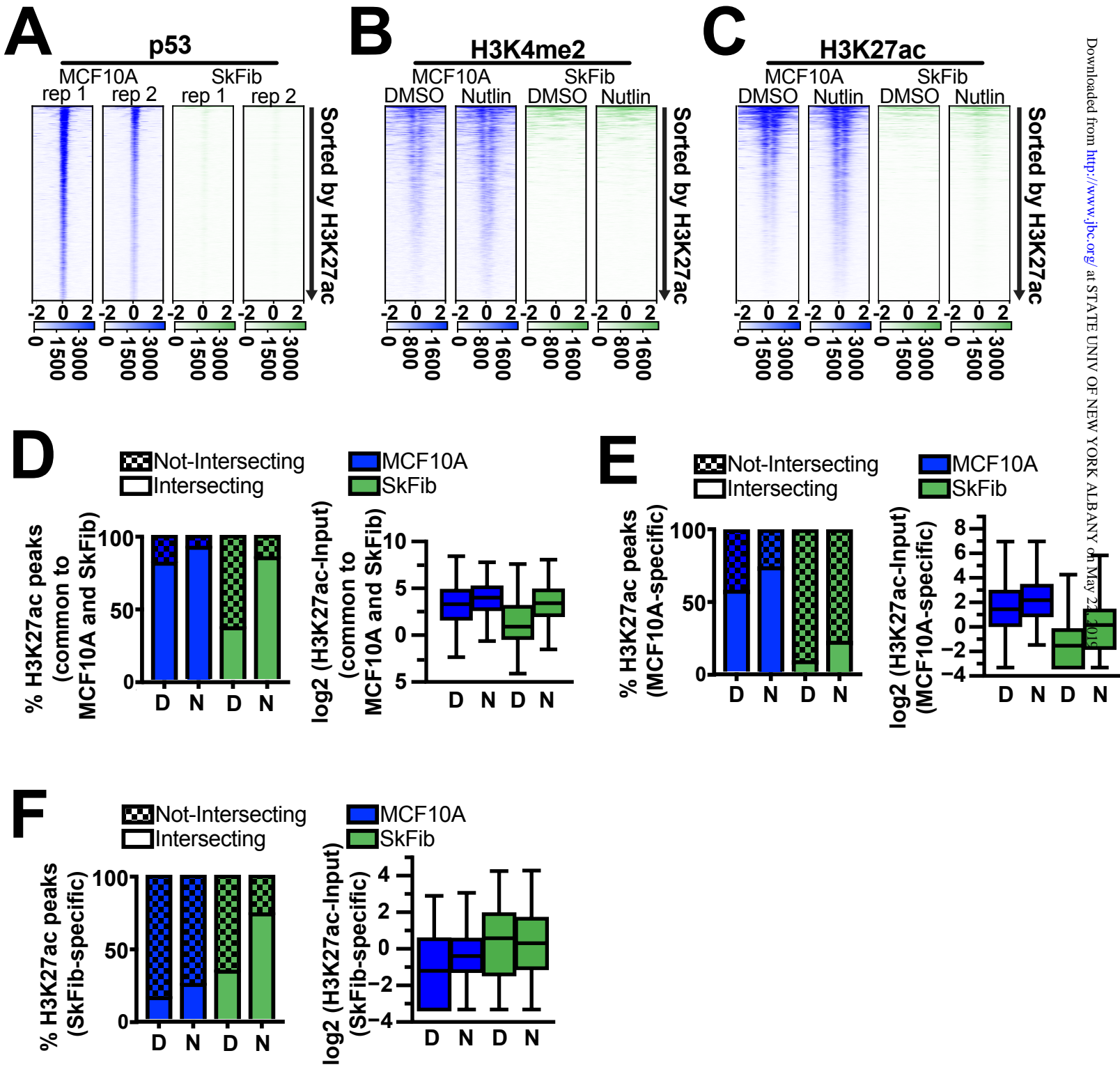
**Figure 2.** **(A)** Venn diagram depicting overlap between significantly-enriched ( $p<0.01$ , MACS v2) Nutlin-3A-induced p53 peaks in MCF10A or SkFib. **(B)** Boxplots depicting enrichment of p53 (input-normalized, log2) at common p53 binding sites found in both MCF10A (blue, left) and SkFib (green, right). **(C)** Fold change ratio of Nutlin-3A/DMSO of common input-subtracted p53 enrichment for MCF10A or SkFib. **(D-E)** Boxplot analysis of the input-subtracted p53 enrichment for MCF10A (blue, left) or SkFib (green, right) for **(D)** MCF10A-specific or **(E)** SkFib-specific-p53 binding sites (right) in response to DMSO (D) or Nutlin-3A (N) treatment. **(F-H)** Chip-qPCR validation of **(F)** the common, **(G)** skin fibroblast specific and **(H)** MCF10A specific p53 target CDKN1A/p21 at p53 binding and non-binding sites. Genome browser view of replicate ChIP-seq data for MCF10A (blue) and SkFib (green) with the location of qPCR primers for p53 binding site and negative region are shown above the qPCR data. qPCR data represent three biological replicates in MCF10A and SkFib cells with either control (scr, non-targeting) or p53-targeting shRNA after 6 hours of Nutlin-3A or DMSO treatment. Statistical analysis was performed by using one-way ANOVA; \*\*\*\* $p<0.0001$ , \*\*\* $p<0.001$ , and \*\* $p<0.01$ .

# Figure 3

**A****B**

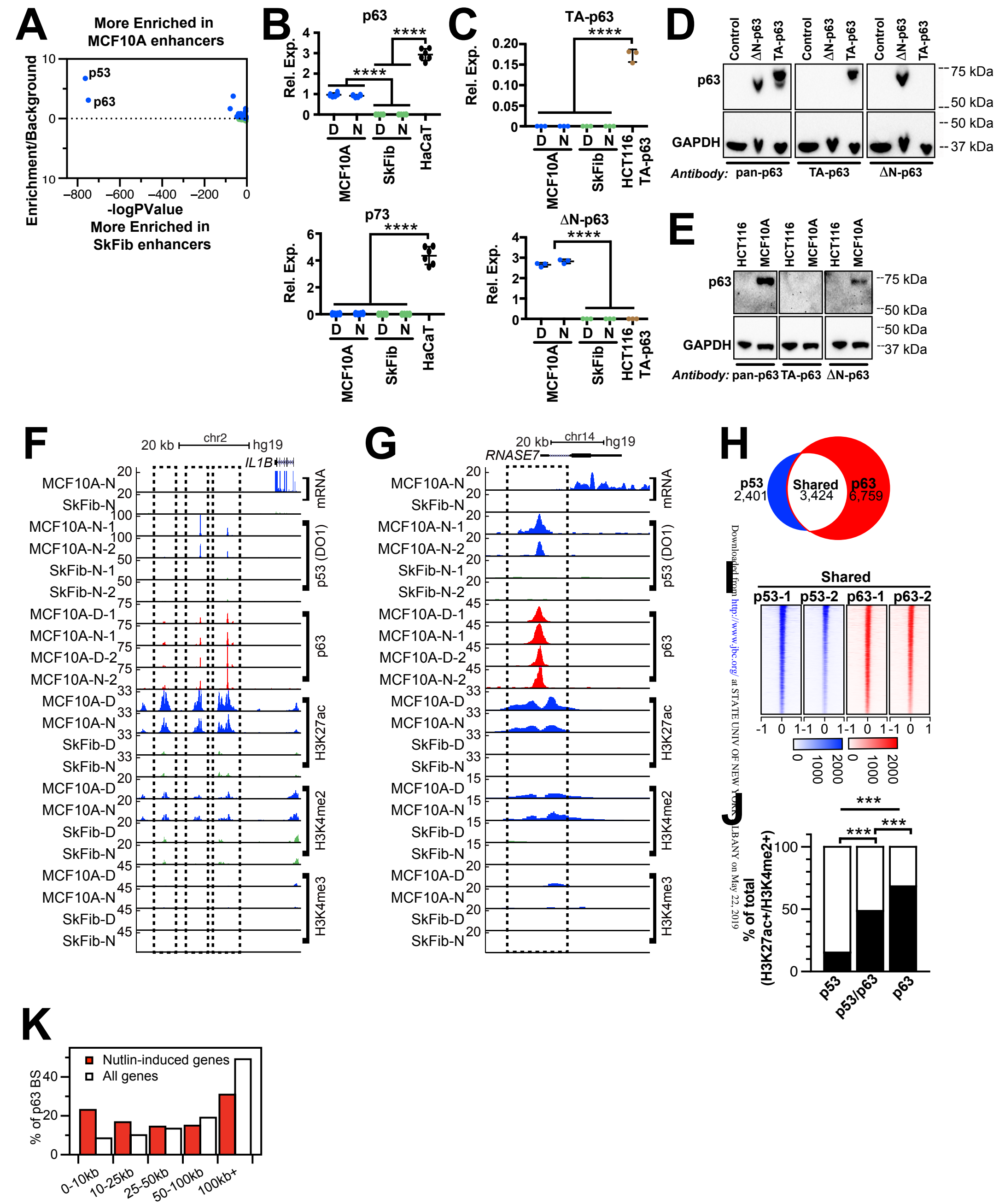
**Figure 3. (A)** Representative UCSC Genome Browser track view of *GDNF* locus, a fibroblast-specific p53 target, in response to DMSO (D) or Nutlin-3A (N) treatment. p53-bound, putative enhancers (H3K27ac+, H3K4me2+, H3K4me3-) illustrated by dashed box for *GDNF* and *TRIM55*, while the putative *GDNF* promoter (H3K27ac/H3K4me2/H3K4me3+) is represented by a solid box. MCF10A-N-1 is biological replicate of MCF10A-N-2, and SkFib-N-1 is biological replicate of SkFib-N-2. The y-axis is scaled to the maximum intensity between MCF10A or SkFib for each feature. **(B)** Representative UCSC Genome Browser track view at the *R/C3* locus, illustrating p53 binding to an MCF10A-specific enhancer signature (H3K27ac/H3K4me2+, H3K4me3-) in response to Nutlin-3A treatment, dashed box. MCF10A-N-1 is biological replicate of MCF10A-N-2, and SkFib-N-1 is biological replicate of SkFib-N-2. The y-axis is scaled to the maximum intensity between MCF10A or SkFib for each feature.

Figure 4



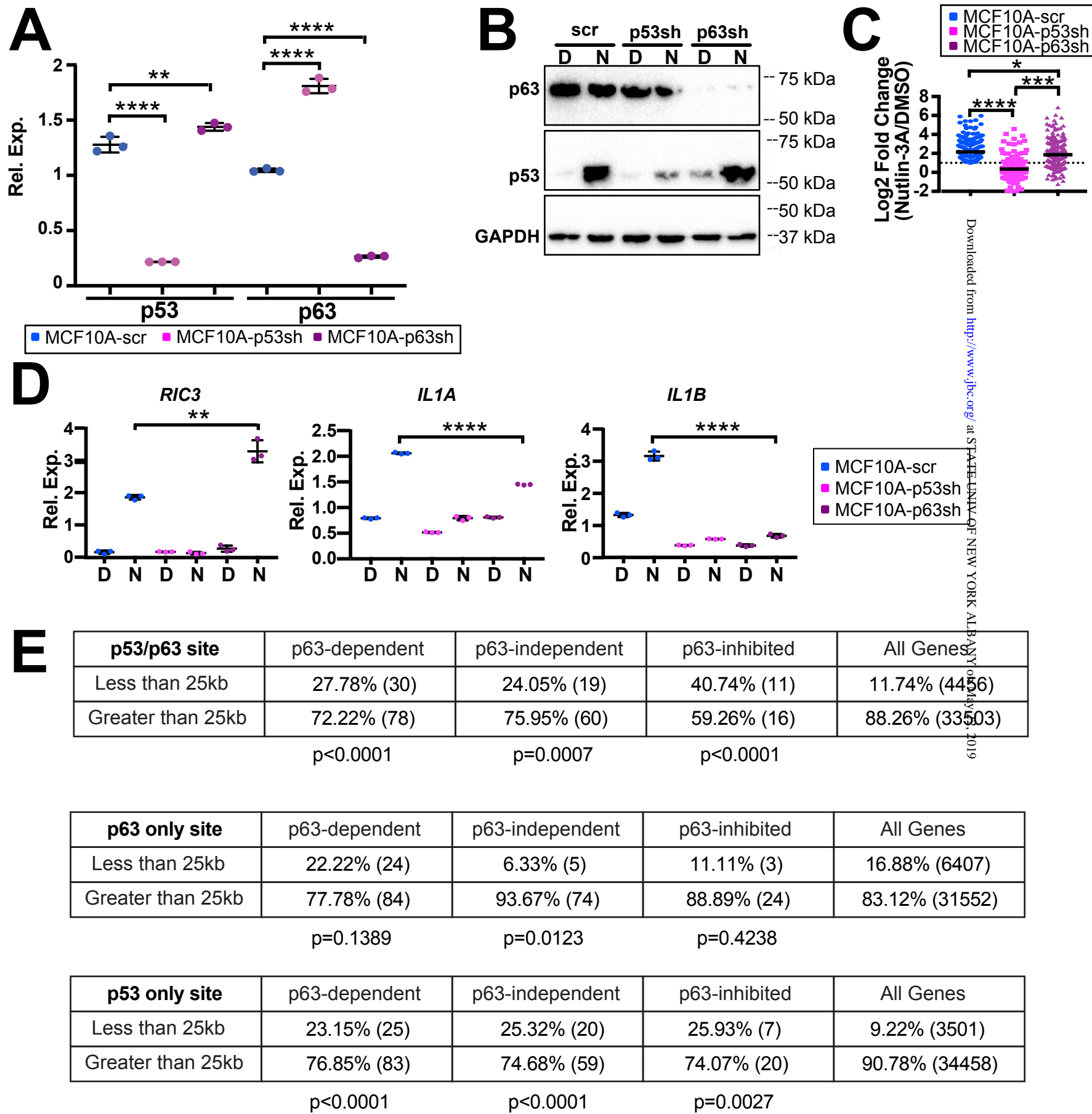
**Figure 4.** **(A)** p53 ChIP-seq enrichment from either MCF10A (blue) or SkFib (green) at MCF10A-specific p53 binding sites. (-/+ 2000 bp from the p53 motif; '-2' indicates 2000bp downstream from the motif, '0' indicates the center of the p53 DNA motif, and '+2' indicates 2000bp upstream of the motif). Two biological replicates for each dataset are shown. **(B)** H3K4me2 and **(C)** H3K27ac enrichment in DMSO or Nutlin-3A-treated MCF10A or SkFib within a 4000-bp window (-/+ 2000 bp from the p53 motif; '-2' indicates 2000bp downstream from the motif, '0' indicates the motif center, and '+2' indicates 2000bp upstream from the motif). **(D-F)** The percentage of intersecting H3K27ac peaks (input-normalized, MACS v2,  $p < 0.01$ ) with p53 peaks (input-normalized, MACS v2,  $p < 0.01$ ) that are **(D)** common to MCF10A and SkFib, **(E)** MCF10A-specific, or **(F)** SkFib-specific in response to DMSO (D) or Nutlin-3A (N) treatment. Adjacent boxplots depict H3K27ac enrichment over a 500bp window from the p53-binding site.

Figure 5



**Figure 5.** **(A)** Homer-derived transcription factor motif enrichment found in MCF10A (top) or SkFib (bottom) specific enhancers (H3K4me2+/H3K27ac+/H3K4me3-). Full list of transcription factor enrichment and facet-specific enhancers are found in Supplemental Table S4. **(B)** qRT-PCR analysis of p53, p63 or p73 of cell lysates from MCF10A, SkFib, HUVEC and HaCaT cells at 6 hours after DMSO (D) or Nutlin-3A (N) treatment. Expressions detected by qRT-PCR are normalized to GAPDH expression. HaCaT cells used as positive control for p63 and p73 expression. Statistical analysis was performed by using one-way ANOVA; \*\*\*p<0.0001. **(C)** qRT-PCR analysis of TA-p63 and ΔN-p63 of cell lysates from MCF10A, SkFib and HCT116-TA-p63 cells. Transiently transfected HCT116 cells with TA-p63 used as a positive control for TA-p63 expression. Statistical analysis was performed by using one-way ANOVA; \*\*\*\*p<0.0001. **(D)** Immunoblotting for p63, TA-p63 and ΔN-p63 of cell lysates from HCT116, HCT116-TAp63 and HCT116-ΔNp63 transiently transfected cells to confirm antibody specificity for different isoforms. **(E)** Immunoblotting for p63, TA-p63 or ΔN-p63 in cell lysates from MCF10A cells. HCT116 cell lysate is used as negative control. **(F)** Representative UCSC Genome Browser track view of the IL1B locus, illustrating three MCF10A-specific putative enhancers bound by p53 and p63 in response to Nutlin-3A treatment (H3K27ac+, H3K4me2+, H3K4me3-; dashed box). The y-axis is scaled to the maximum intensity for each data set. MCF10A-D-1 is biological replicate of MCF10A-D-2, MCF10A-N-1 is biological replicate of MCF10A-N-2, and SkFib-N-1 is biological replicate of SkFib-N-2. **(G)** Representative UCSC Genome Browser track view of the RNASE7 locus, illustrating a MCF10A-specific putative enhancer bound by p53 and p63 in response to DMSO (D) or Nutlin-3A (N) treatment (H3K27Ac+, H3K4me2+, H3K4me3-; dashed box). The y-axis is scaled to the maximum intensity for each data set. MCF10A-D-1 is biological replicate of MCF10A-D-2, MCF10A-N-1 is biological replicate of MCF10A-N-2, and SkFib-N-1 is biological replicate of SkFib-N-2. **(H)** Venn diagram representation of overlapping p53 and p63 ChIP-seq peaks (input-normalized, p53/p63 motif-positive, MACS v2, p<0.01) in MCF10A when treated with Nutlin-3A. **(I)** Heatmap plots of p53 and p63 enrichment at shared binding sites in replicate MCF10A cells within a 2000-bp window (-/+ 1000 bp from the peak center) in response to Nutlin-3A treatment. **(J)** The percentage of intersecting H3K27ac/H3K4me2+ peaks (input-normalized, MACS v2, p<0.01) with p53 only, p63 only, or p53/p63 peaks observed in MCF10A cells (input-normalized, MACS v2, p<0.01). **(K)** The percentage of p63 binding sites observed in MCF10A cells at varying distances to the near- est TSS of all RefSeq genes (white) or Nutlin-3A induced genes (red).

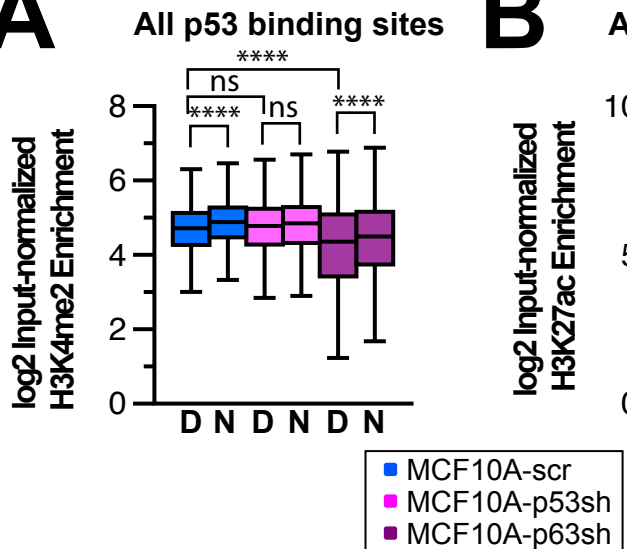
Figure 6



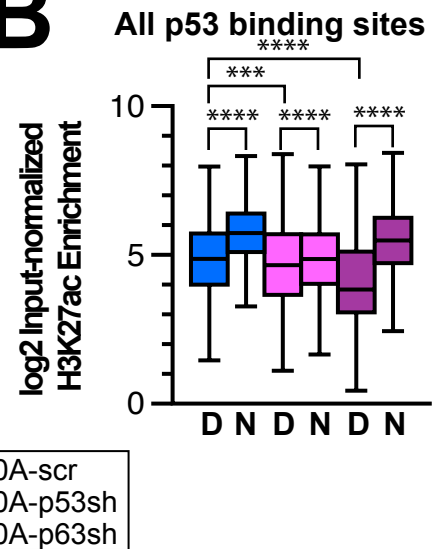
**Figure 6.** **(A)** qRT-PCR analysis of p53 and p63 in response to p63 knockdown in MCF10A cells stably expressing shRNA to p63 or a non-targeting control shRNA (scr) after 6 hours of DMSO (D) or Nutlin-3A (N) treatment. Target gene expression is normalized to GAPDH for qRT-PCR analysis. Statistical analysis was performed by using one-way ANOVA; \*\*\*\*p<0.0001 and \*\*\*p<0.001. **(B)** Immunoblotting for p53, p63, and GAPDH in MCF10A cells stably expressing shRNA to p53, p63 or a non-targeting control shRNA (scr) after 6 hours of DMSO (D) or Nutlin-3A (N) treatment. This immunoblot image is an uncropped version of Figure 1J. **(C)** RNA-seq analysis of MCF10A-specific, Nutlin-3A-induced genes in MCF10A cells expressing shRNA targeting either a non-targeting control (scr), p53, or p63. Data are graphed as fold-change (Nutlin-3A/DMSO, log<sub>2</sub>, median in black). Statistical analysis was performed by using one-way ANOVA. \*\*\*\*p<0.0001, \*\*\*p<0.001 and \*p<0.05. **(D)** qRT-PCR analysis of MCF10A-specific Nutlin-3A-induced genes, *R1C3*, *IL1A* and *IL1B*. Expression is normalized to GAPDH expression. Error bars represent SEM; \*\*\*\*p<0.0001 and \*\*p<0.01, calculated by Student's t-test. **(E)** The percent of p53, p63, and p53/p63 co-bound sites relative to the three classes of p63-regulated p53 gene targets (p63-dependent, p63-independent, and p63-inhibited) in binned distance regions (under 25kb and over 25kb). Statistics represent chi-square test using the distance of each binding site class to non-regulated genes.

Figure 7

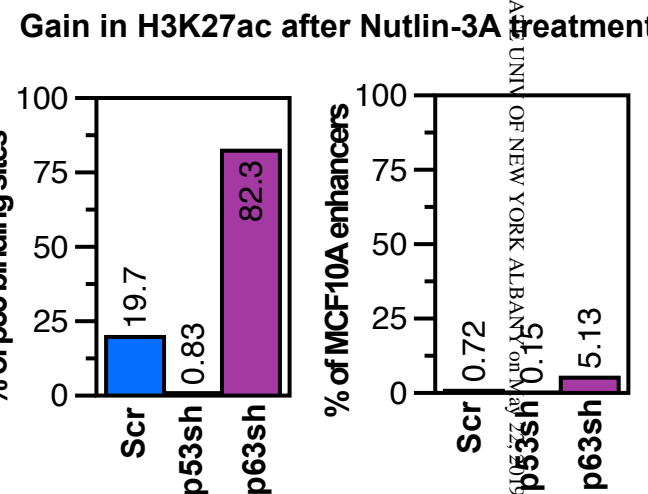
A



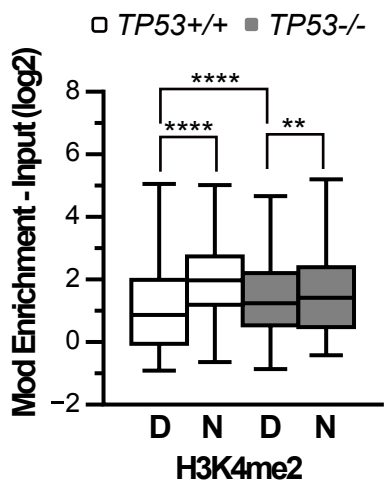
B



C



D



E

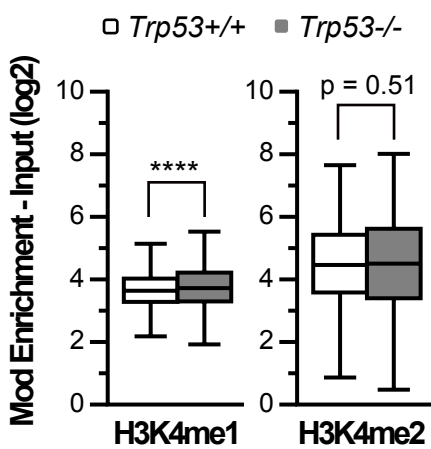


**Figure 7.** **(A)** H3K4me2 enrichment (Input-subtracted H3K4me2, -/+ 250bp from p53 motif center) at p53 binding sites in MCF10A cells expressing control (scr), p53, or p63-targeted shRNA in response to DMSO or Nutlin-3A treatment. Statistical analysis was performed by using one-way ANOVA. \*\*\*\*p<0.0001 **(B)** H3K27ac enrichment at p53 binding sites in MCF10A cells expressing the represented shRNA molecules after 6hours of DMSO (D) or 5uM Nutlin-3A (N) treatment. Statistical analysis was performed by using one-way ANOVA. \*\*\*\*p<0.0001 and \*\*\*p<0.001. **(C)** Bar graph displaying the number of p53 binding sites (left) or total cellular complement of H3K27ac+/H3K4me2+/H3K4me3- enhancers with more than 2-fold change in H3K27ac enrichment after Nutlin-3A treatment of MCF10 cells expressing the indicated shRNA. **(D)** H3K4me2 enrichment at p53 binding sites (25) in HCT116 *TP53*+/- or -/- cells in response to DMSO or Nutlin-3A treatment. Statistical analysis was performed by using one-way ANOVA. \*\*\*\*p<0.0001 and \*\*p<0.01. **(E)** H3K4me1 and H3K4me2 enrichment at p53 binding sites (85) in *Trp53*+/- or *Trp53*-/- mouse embryonic fibroblasts.

Figure 8

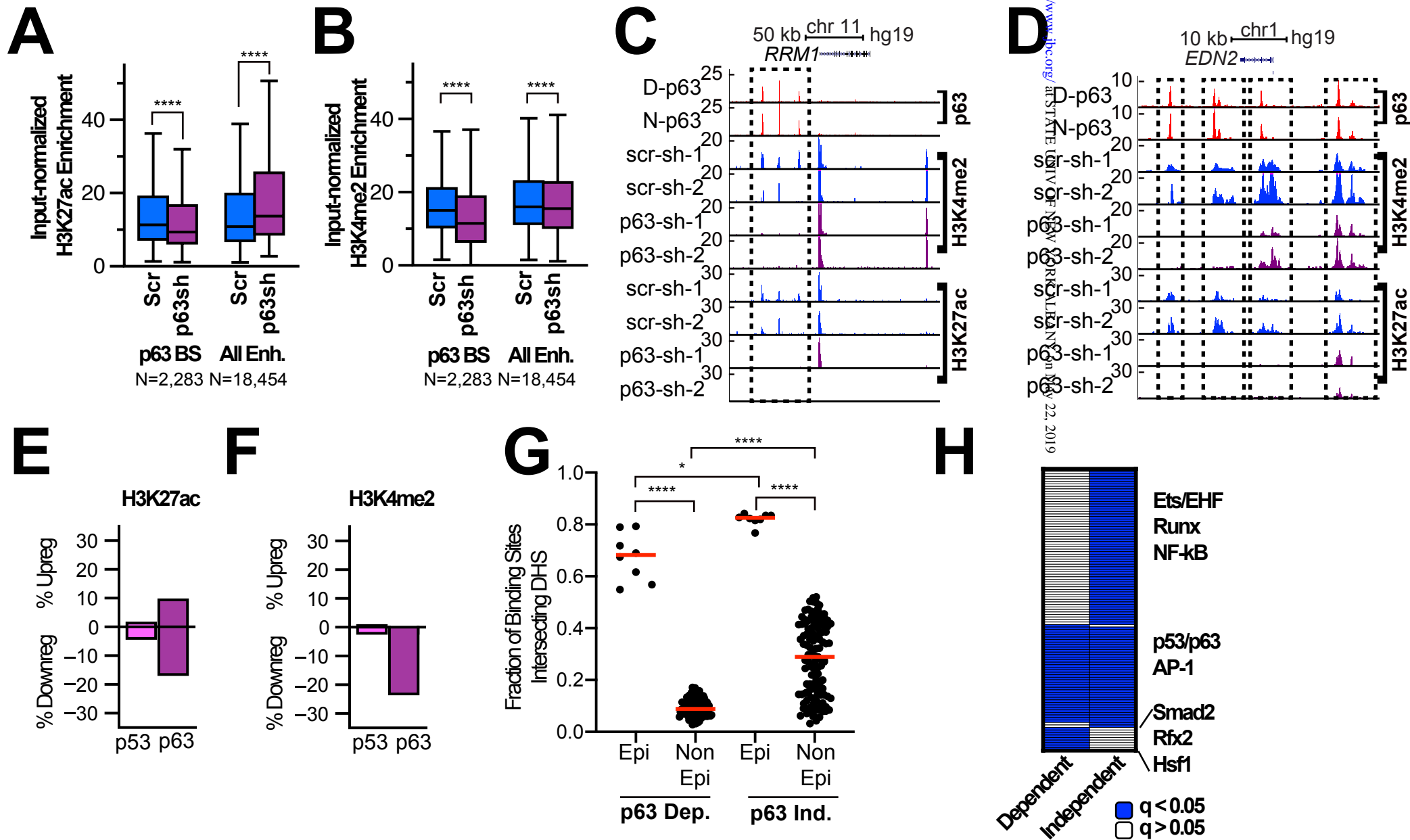


**Figure 8.** (A-B) Input-subtracted (A) H327ac or (B) H3K4me2 enrichment at p63 binding sites (left, -/+ 250bp from p63 peak center) or at all remaining enhancers (H3K27ac+, H3K4me2+, H3K4me3-, right) in MCF10A cells expressing non-targeting (Scr) or p63 shRNA. (C) Representative UCSC Genome Browser track view of the RRM1 locus, illustrating three MCF10A-specific putative enhancers bound by p63 that are lost in response to p63 depletion (H3K27ac+, H3K4me2+, H3K4me3-; dashed box). (D) Representative UCSC Genome Browser track view of the *EDN2* locus, illustrating three MCF10A-specific putative enhancers bound by p63 that are lost in response to p63 depletion (H3K27ac+, H3K4me2+, H3K4me3-; three separate dashed box). The y-axis is scaled to the maximum intensity for each data set. (E) Bar graphs depicting the percent of p63 peaks that show 2-fold gains or losses of H3K27ac (left) or H3K4me2 (right) in response to either p53 or p63 depletion relative to non-targeting control shRNA. (F) The number of p63-sensitive, H3K4me2-marked enhancers (out of 1496 total) overlapping DNAse hypersensitive sites (DHS) across epithelial and non-epithelial cell types analyzed by the ENCODE project. Error bars represent the median and 95% confidence interval. (G) Jitter plot depicting the fraction of p63-dependent or independent enhancers overlapping regions of DNAse hypersensitive sites (DHS) across both epithelial and non-epithelial cell lines as assayed by the ENCODE project. (H) Heatmap of k-means (k=3) clustered Bonferroni-corrected P-values (q-values) for motif enrichment found at p63-dependent or independent enhancers. Blue represents adjusted p-values less than 0.05 while white represents adjusted p-values greater than 0.05. A full list of motifs and their enrichment statistics can be found in Supplemental Table S7.

**Control of p53-dependent transcription and enhancer activity by the p53 family member p63**

Gizem Karsli Uzunbas, Faraz Ahmed and Morgan A Sammons

*J. Biol. Chem.* published online May 21, 2019

---

Access the most updated version of this article at doi: [10.1074/jbc.RA119.007965](https://doi.org/10.1074/jbc.RA119.007965)

Alerts:

- [When this article is cited](#)
- [When a correction for this article is posted](#)

[Click here](#) to choose from all of JBC's e-mail alerts